Plant Communications
Research Article

CellPress
Partner Journal

Brassinosteroids promote thermotolerance through releasing BIN2-mediated phosphorylation and suppression of HsfA1 transcription factors in *Arabidopsis*

Jinyu Luo[1,2,3], Jianjun Jiang[2], Shiyong Sun[2] and Xuelu Wang[2,3,*]

[1]College of Life Science and Technology, Huazhong Agricultural University, Wuhan 430070, China

[2]State Key Laboratory of Crop Stress Adaptation and Improvement, Henan University, Kaifeng 475004, China

[3]Sanya Institute of Henan University, Sanya 572025, China

***Correspondence: Xuelu Wang (xueluw@henu.edu.cn)**

https://doi.org/10.1016/j.xplc.2022.100419

ABSTRACT

High temperature adversely affects plant growth and development. The steroid phytohormones brassinosteroids (BRs) are recognized to play important roles in plant heat stress responses and thermotolerance, but the underlying mechanisms remain obscure. Here, we demonstrate that the glycogen synthase kinase 3 (GSK3)-like kinase BRASSINOSTEROID INSENSITIVE2 (BIN2), a negative component in the BR signaling pathway, interacts with the master heat-responsive transcription factors CLASS A1 HEAT SHOCK TRANSCRIPTION FACTORS (HsfA1s). Furthermore, BIN2 phosphorylates HsfA1d on T263 and S56 to suppress its nuclear localization and inhibit its DNA-binding ability, respectively. BR signaling promotes plant thermotolerance by releasing the BIN2 suppression of HsfA1d to facilitate its nuclear localization and DNA binding. Our study provides insights into the molecular mechanisms by which BRs promote plant thermotolerance by strongly regulating HsfA1d through BIN2 and suggests potential ways to improve crop yield under extreme high temperatures.

Key words: brassinosteroids, thermotolerance, BIN2, HsfA1d, phosphorylation

Luo J., Jiang J., Sun S., and Wang X. (2022). Brassinosteroids promote thermotolerance through releasing BIN2-mediated phosphorylation and suppression of HsfA1 transcription factors in *Arabidopsis*. Plant Comm. **3**, 100419.

INTRODUCTION

High temperatures above optimum growing temperature have detrimental impacts on plant vegetative growth and reproduction (Bita and Gerats, 2013; Sage et al., 2015; Zhao et al., 2017). As sessile organisms, plants have developed intricate systems to cope with heat shock (HS). Several studies have reported multiple plant HS stress sensors localized from the plasma membrane to the nucleus (Hayes et al., 2021). HS response (HSR) genes are elicited by plant HS stress sensors through various pathways, including the cyclic nucleotide-gated calcium channel (CNGC)-calcium-calmodulin pathway (Liu et al., 2003, 2008; Saidi et al., 2009; Finka et al., 2012; Cui et al., 2020), reactive oxygen species (ROS) signaling pathways in chloroplasts and mitochondria (Volkov et al., 2006; Xuan et al., 2010; Babbar et al., 2020), intracellular accumulation of hydrogen peroxide (H_2O_2) and nitric oxide (NO) that transduce the early HSRs (Volkov et al., 2006; Wang et al., 2014b), and heat-denatured proteins in the cytosol and endoplasmic reticulum that induce the unfolded protein response (UPR) (Sugio et al., 2009; Deng et al., 2011; Neill et al., 2019). Many of these pathways strongly activate a class of HEAT SHOCK TRANSCRIPTION FACTORS (HSFs), which are considered to play conserved and central roles in eukaryotic HSRs (Li et al., 2018; Andrasi et al., 2021). The activated HSFs bind to *cis*-acting DNA elements, known as heat shock elements (HSEs; 5′-nGAAnnTTCn-3′ or 5′-nTTCnnGAAn-3′), to regulate the expression of hundreds of HS-inducible genes, including heat shock proteins (HSPs) (Pelham, 1982; Bienz and Pelham, 1987; Guo et al., 2008).

The *Arabidopsis* genome contains 21 HSF-encoding genes that are grouped into A, B, and C classes and further divided into 14 groups (A1–A9, B1–B4, and C1) according to their protein domain structure and phylogenetic relationships (Scharf et al., 2012; Guo

Published by the Plant Communications Shanghai Editorial Office in association with Cell Press, an imprint of Elsevier Inc., on behalf of CSPB and CEMPS, CAS.

This is an open access article under the CC BY-NC-ND license (http://creativecommons.org/licenses/by-nc-nd/4.0/).

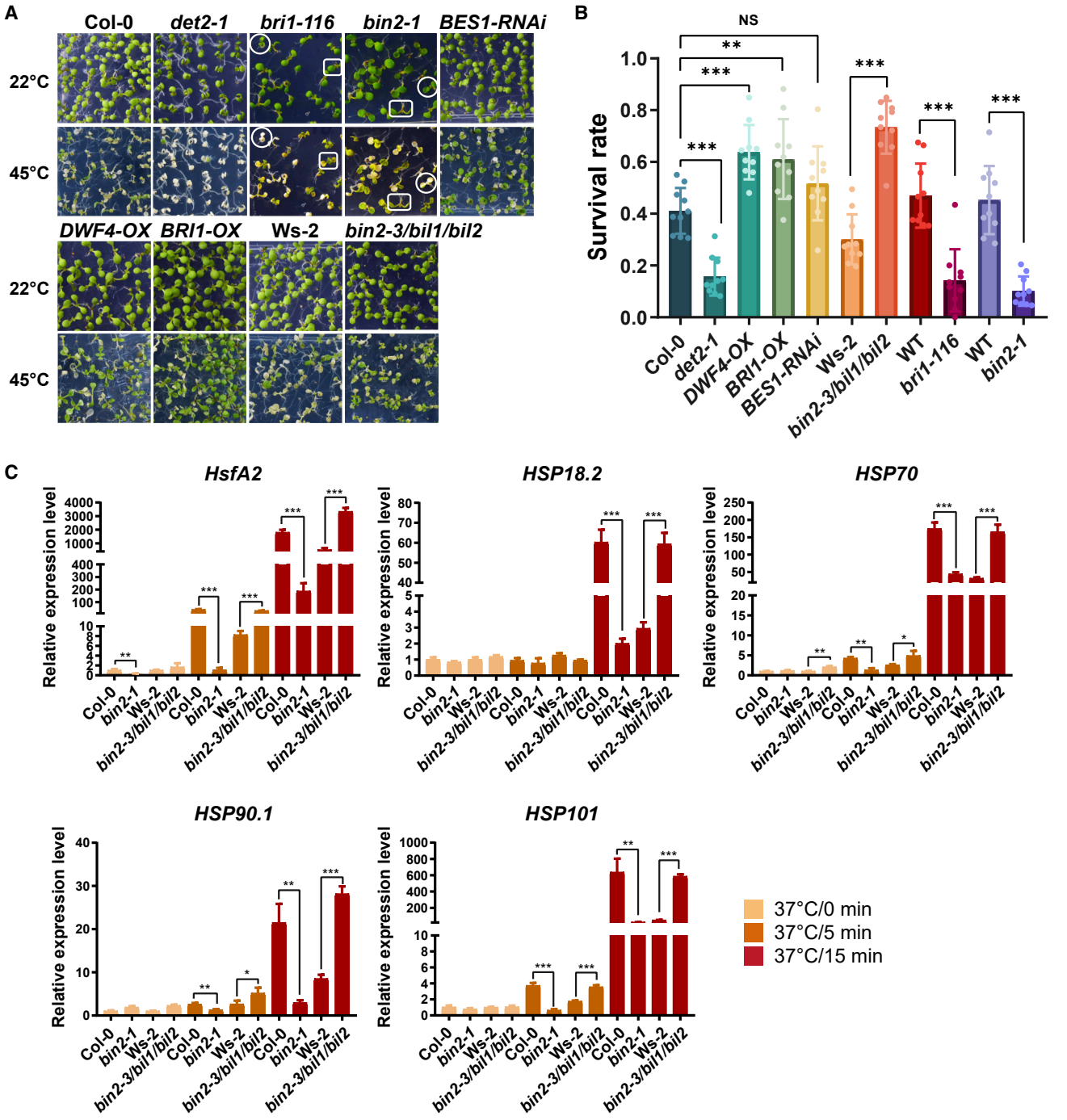

Figure 1. BR signaling is involved in thermotolerance

(A) Basal thermotolerance phenotypes of BR-related *Arabidopsis* mutants. Nine-day-old seedlings were treated with 45°C for 105 min, followed by a 4-day recovery at 22°C. The upper panel shows the plants before heat treatment, and the bottom panel shows the plants after heat treatment and recovery. Surviving plants were defined as those that were able to maintain fresh and green leaves and form new leaves. *bri1-116* and *bin2-1* are progenies of heterozygous materials because of homozygous infertility. The white circles indicate representative homozygous mutant seedlings, and the white squares indicate representative WT seedlings. For the recessive mutant *bri1-116*, the WT includes homozygous wild type (*BRI1*/*BRI1*) and heterozygous wild type (*BRI1*/*bri1-116*). For the semi-dominant mutant *bin2-1*, the WT indicates the homozygous wild type (*BIN2*/*BIN2*).

(B) Statistical results of thermotolerance phenotypes. Survival rates were calculated after recovery following 45°C treatment. Each plate was considered to be one biological replicate, and at least 10 biological replicates collected from three to four independent experiments were used for statistical analysis of survival rate. Data are mean ± SD (n = 10). p values were determined using unpaired t tests (**p < 0.01 and ***p < 0.001; non-significant [NS], p > 0.05).

(legend continued on next page)

et al., 2016). Thermotolerance phenotypes of a number of HSF mutants in response to HS indicate that three members of the HsfA1s, HsfA1a, HsfA1b, and HsfA1d, are the early and master transcriptional activators required for HSRs (Liu et al., 2011; Yoshida et al., 2011; Liu and Charng, 2013). The triple mutants *hsfA1a/b/d* are dramatically defective in HS tolerance compared with their various double mutants, suggesting the functional redundancy of these genes (Yoshida et al., 2011). The activated HsfA1s can induce the expression of *HSPs* as well as other *HSFs* such as *HsfA2*, which encodes a key early transcription factor, to strongly amplify HSRs (Nishizawa et al., 2006; Liu et al., 2011; Nishizawa-Yokoi et al., 2011; Friedrich et al., 2021). In mammalian cells, HSFs are activated by release from a chaperone complex followed by trimerization, nuclear translocation, and binding to HSEs, which require post-translational modifications of HSFs (Chu et al., 1996; Anckar and Sistonen, 2011; Gomez-Pastor et al., 2018). Much evidence indicates that similar mechanisms may exist in plants and that post-translational modifications of HsfA1s are also important for their activation in *Arabidopsis* (Liu et al., 2007; Yamada et al., 2007; Evrard et al., 2013), but the underlying biochemical mechanism remains largely unknown.

A number of studies have indicated that brassinosteroids (BRs), a class of growth-promoting steroid hormones, play an important role in plant thermotolerance (Yang et al., 2011; Sun et al., 2015; Liu et al., 2018; Fang et al., 2020). Treatment with 24-epibrassinolide (eBL), a synthetic analog of brassinolide, increases the survival rates of *Brassica napus*, tomato, and *Arabidopsis* seedlings under heat stress (Dhaubhadel et al., 1999; Kagale et al., 2007). BRs are perceived by the plasma membrane–localized leucine-rich repeat receptor-like kinase BRASSINOSTEROID INSENSITIVE 1 (BRI1) (Li and Chory, 1997). Without BRs, BRI1 is kept inactive by its carboxyl terminus and the negative regulator BRI1 KINASE INHIBITOR1 (BKI1) (Wang et al., 2005b, 2011, 2014a, 2017; Wang and Chory, 2006; Jiang et al., 2015a). BR binding to the extracellular domain of BRI1 triggers association with its co-receptor BRI1-ASSOCIATED RECEPTOR KINASE1 (BAK1) and intracellular kinase trans-phosphorylation, leading to release of BKI1 inhibition (Li et al., 2002; Wang et al., 2005a, 2005b, 2011; Wang and Chory, 2006; Jiang et al., 2013). The activated BRI1 then phosphorylates the BR SIGNALING KINASES (BSKs) and CONSTITUTIVE DIFFERENTIAL GROWTH 1 (CDG1), leading to phosphorylation and activation of the phosphatase BRI1 SUPRRESSOR1 (BSU1) (Mora-García et al., 2004; Tang et al., 2008; Kim et al., 2011; Yang et al., 2011). The phosphorylated BSU1 dephosphorylates and inhibits BIN2 to release its phosphorylation and inhibition of the central downstream transcription factors BRI1 EMS SUPPRESSOR1 (BES1) and its homologs, which directly regulate BR-responsive genes involved in many developmental processes (Li and Nam, 2002; Yin et al., 2002; Wang et al., 2013; Cheng et al., 2014; Jiang et al., 2015b; Hao et al., 2016; Qiao et al., 2017; Yang et al., 2017; Yang and Wang, 2017; Hu et al., 2020). Although eBL treatment has been shown to promote thermotolerance, the molecular mechanism by which BR signaling regulates plant HSRs has not been elucidated.

In this study, we examined the responses of various BR-related mutants to HS and found that early BR signaling, specifically BIN2 and its upstream signaling components, is involved in BR-mediated thermotolerance. We found that BIN2 interacts with and phosphorylates all four members of the HsfA1s. Phosphorylation of HsfA1d on T263 and S56 by BIN2 can inhibit the nuclear localization and DNA-binding ability of HsfA1d, respectively. Genetic and phenotypic analyses provided evidence that BIN2 functions upstream of HsfA1d to inhibit thermotolerance. Furthermore, BR signaling promotes plant thermotolerance by regulating HsfA1d subcellular localization and DNA-binding ability through BIN2. Our study therefore provides insights into the genetic and biochemical mechanisms by which plant thermotolerance is regulated through the integration of phytohormone signaling and HS-responsive signaling pathways.

RESULTS

BR early signaling components mediate BR-regulated plant thermotolerance

To investigate whether BRs promote plant thermotolerance through their signaling pathway, we performed basal and acquired thermotolerance assays using the BR biosynthesis-deficient mutant *det2-1* and the BR signaling-attenuated mutants *bri1-116* and *bin2-1*. Seedlings were treated with heat stresses as indicated in supplemental figure 1B, followed by a 4-day recovery period at 22°C, after which plant survival was assessed, defined as the ability to maintain fresh and green leaves and to form new leaves, thus indicating thermotolerance (supplemental figure 1A and 1B). We found that *det2-1*, *bri1-116*, and *bin2-1* showed reduced survival rates compared with their corresponding wild type (WT) in both basal and acquired thermotolerance assays (supplemental figure 1A and 1C). We next performed basal thermotolerance assays using more BR biosynthesis and signaling mutants, including *DWF4-OX*, *BRI1-OX*, *bin2-3/bil1/bil2*, *bes1-D*, and *BES1-RNAi*. Nine-day-old seedlings were exposed to 45°C high temperature for 105 min, followed by a 4-day recovery period at 22°C, after which the survival rates were assessed to indicate basal thermotolerance (Figure 1A). We found that all of the mutants with enhanced BR synthesis and signaling, including *DWF4-OX*, *BRI1-OX*, and the GSK3 triple loss-of-function mutant *bin2-3/bil1/bil2*, showed increased survival rates compared with their corresponding WT (Figures 1A and 1B). By contrast, the BR-deficient mutant *det2-1*, the signaling-attenuated mutant *bri1-116*, and the gain-of-function mutant *bin2-1* had lower survival rates compared with their corresponding controls (Figures 1A and 1B). However, the survival rates of *BES1-RNAi* and *bes1-D* did not differ significantly from that of the WT (Figures 1A and 1B; supplemental figure 1D and 1E). These results suggest that BIN2 and its upstream signaling components play major roles in BR-mediated thermotolerance. To further test the role of BIN2 in plant HSRs, we measured the relative expression levels of HSR marker genes in the

(C) Expression levels of HSR genes in *bin2-3/bil1/bil2*, *bin2-1*, and their corresponding WT seedlings under normal and heat stress conditions. Nine-day-old seedlings grown on half strength MS plates at 22°C were harvested before and after 37°C treatment for the indicated time. Total RNA extracted from seedlings was used for qRT-PCR analysis. The expression levels were normalized to WT before heat stress treatment (0 min). Data are mean ± SD (n = 3). p values were determined using unpaired t tests (*$p < 0.05$, **$p < 0.01$, and ***$p < 0.001$).

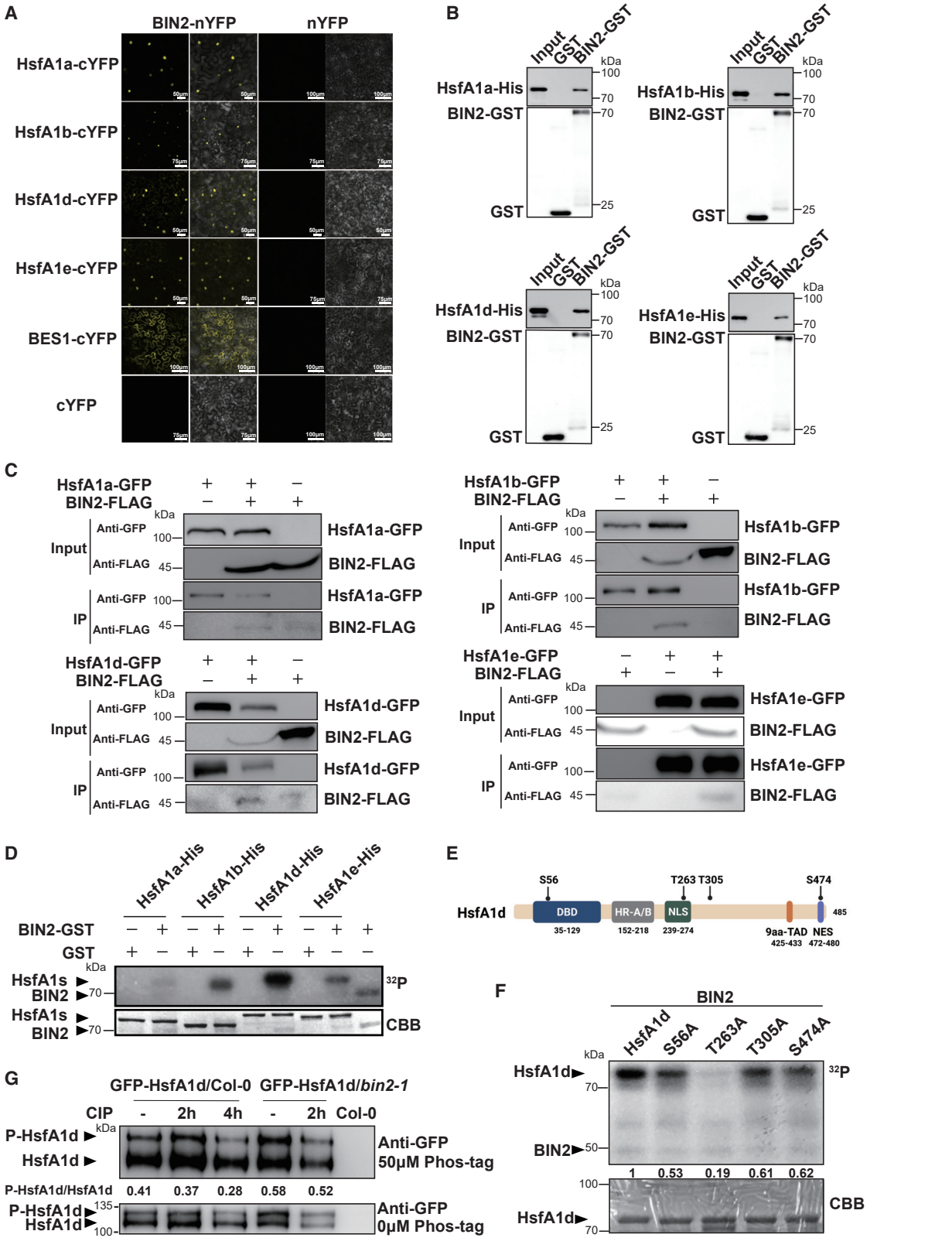

Figure 2. BIN2 interacts with HsfA1s and phosphorylates HsfA1d *in vitro* and *in vivo*

(A) BiFC assays for the interactions between BIN2 and HsfA1a, HsfA1b, HsfA1d, and HsfA1e in *Nicotiana benthamiana*. BES1 was used as a positive control.

(legend continued on next page)

bin2-3/bil1/bil2 and *bin2-1* seedlings after short-term heat treatment. We found that the heat-induced expression levels of HSR genes were significantly higher in the *bin2-3/bil1/bil2* triple mutant but lower in *bin2-1* compared with their WT (Figure 1C), indicating that BIN2 may play a pivotal role in mediating the crosstalk between BR and heat shock signaling pathways.

BIN2 physically interacts with HsfA1s and phosphorylates HsfA1d *in vitro* and *in vivo*

The human glycogen synthase kinase 3β (GSK3β), a homolog of plant GSK3s (Li and Nam, 2002), has been shown to phosphorylate the master HSR regulator HEAT SHOCK TRANSCRIPTION FACTOR 1 (HsHSF1) (Chu et al., 1996). Considering that HsfA1s function as central downstream transcriptional activators in *Arabidopsis* HSR (Yoshida et al., 2011), as well as the conservation of both HSF and GSK3 in humans and plants (supplemental figure 2), we asked whether plant GSK3 can interact with and regulate HsfA1s. We first used bimolecular fluorescence complementation (BiFC) assays in *Nicotiana benthamiana* pavement cells to investigate this possibility and found that BIN2 can interact with all members of the HsfA1s, including HsfA1a, HsfA1b, HsfA1d, and HsfA1e (Figure 2A). We next performed *in vitro* GST pull-down assays using recombinant BIN2-GST and HsfA1-His proteins purified from *Escherichia coli*. We found that BIN2-GST could pull down all the HsfA1a-, HsfA1b-, HsfA1d-, and HsfA1e-His proteins (Figure 2B). To test this interaction *in vivo*, we generated *BIN2-FLAG*, *HsfA1a-GFP*, *HsfA1b-GFP*, *HsfA1d-GFP*, and *HsfA1e-GFP* transgenic *Arabidopsis* driven by a strong *35S* promoter and crossed *BIN2-FLAG* with GFP-tagged HsfA1 lines to obtain progenies expressing both proteins for co-immunoprecipitation. After immunoprecipitation with GFP beads, we found that BIN2-FLAG protein could be co-purified with HsfA1b-GFP and HsfA1d-GFP proteins in planta and slightly co-purified with HsfA1a-GFP and HsfA1e-GFP (Figure 2C). Taken together, these results demonstrated that BIN2 could physically interact with HsfA1b/d and slightly interact with HsfA1a/e.

BIN2 has been reported to participate in a number of plant developmental and stress responses by phosphorylating several transcription factors (Cheng et al., 2014; Youn and Kim, 2015; Jiang et al., 2019; Ye et al., 2019; He et al., 2021). Therefore, we performed *in vitro* kinase assays to test whether the HsfA1s can be phosphorylated by BIN2. We incubated recombinant BIN2-GST and HsfA1-His proteins, as well as ^{32}P-labelled ATP, and found ^{32}P autoradiographic signals on all HsfA1 proteins, with the highest signal observed for HsfA1d (Figure 2D), suggesting that BIN2 can phosphorylate all HsfA1s with a preference for HsfA1d *in vitro*. Overexpression of *HsfA1d* has been reported to confer thermotolerance in many plant species (Higashi et al., 2013; Shah et al., 2020), and HsfA1d can directly upregulate *HsfA2* expression (Nishizawa-Yokoi et al., 2011). Therefore, we focused our study on HsfA1d. To identify potential HsfA1d phosphorylation sites, we first performed mass spectrometry after *in vitro* phosphorylation and identified a number of residues, including S56 located in the DNA-binding domain, T263 in the nuclear localization signal (NLS), T305 between the NLS and the transcription activation domain, and S474 in the nuclear export signal (Figure 2E and supplemental figure 3). We next mutated these potential phosphorylation sites into Ala to perform *in vitro* phosphorylation assays. We found that HsfA1d^{S56A}, HsfA1d^{T305A}, and HsfA1d^{S474A} proteins showed slight reductions in phosphorylation by BIN2, whereas phosphorylation was almost abolished for HsfA1d^{T263A} proteins (Figure 2F), suggesting that T263 is a major phosphorylation site for BIN2. To further investigate whether BIN2 phosphorylates HsfA1d *in vivo*, we created *GFP-HsfA1d* transgenic *Arabidopsis* plants in the Col-0 and *bin2-1* backgrounds to purify GFP-HsfA1d proteins and perform Phos-tag mobility shift assays. We found that GFP-HsfA1d protein separated into two forms, and the relative amount of the slow-migrating form, which indicates phosphorylation, increased in the *bin2-1* background compared with the Col-0 background (Figure 2G). Moreover, incubation of the GFP-HsfA1d protein with calf intestinal alkaline phosphatase (CIP) eliminated the slow-migrating form of HsfA1d (Figure 2G). To further verify the phosphorylation sites of HsfA1d by BIN2 *in vivo*, we immunoprecipitated GFP-HsfA1d protein from the *GFP-HsfA1d/bin2-1* transgenic plants to perform mass spectrometry and identified six residues, including the T263 site (supplemental figure 4). These results indicated that BIN2 phosphorylates HsfA1d *in vitro* and *in vivo*, and T263 is a key phosphorylation site of HsfA1d by BIN2.

BIN2 inhibits nuclear translocation of HsfA1d by phosphorylating T263

Because T263 is located in an NLS (Figure 2E), we asked whether the phosphorylation of HsfA1d on the T263 residue by BIN2 can

(B) GST pull-down assays for the interactions between BIN2-GST and His-tagged HsfA1 proteins. GST and BIN2-GST recombinant proteins were used as baits, and their loading amounts are shown in the bottom panel. The input and pull-down signals of prey proteins HsfA1a-His, HsfA1b-His, HsfA1d-His, and HsfA1e-His are shown in the upper panel.

(C) Co-immunoprecipitation assays for the interaction between BIN2-FLAG and HsfA1a-GFP, HsfA1b-GFP, HsfA1d-GFP, or HsfA1e-GFP. The proteins were extracted from the transgenic *Arabidopsis* plants and immunoprecipitated with GFP beads. The input and co-immunoprecipitated proteins were subjected to immunoblot analysis with anti-FLAG or anti-GFP antibody as indicated.

(D) *In vitro* phosphorylation of His-tagged HsfA1a, HsfA1b, HsfA1d, and HsfA1e proteins by BIN2-GST kinase. The phosphorylation level is indicated by the autoradiography of ^{32}P transferred from ^{32}P-ATP to protein. The bottom image shows Coomassie brilliant blue (CBB) staining.

(E) A schematic diagram shows the amino acid sequence features and potential phosphorylation sites identified by mass spectrometry analysis. DBD, DNA-binding domain; HR-A/B, oligomerization domain; NLS, nuclear localization signal; 9 aa-TAD, transactivation domain; NES, nuclear export signal. Black dots indicate the phosphorylation sites identified by mass spectrometry *in vitro*.

(F) *In vitro* phosphorylation assays of His-tagged HsfA1d, HsfA1d^{S56A}, HsfA1d^{T263A}, HsfA1d^{T305A}, and HsfA1d^{S474A} proteins by BIN2-His kinase. The phosphorylation level is indicated by the autoradiography of ^{32}P transferred from ^{32}P-ATP to protein. The bottom image shows CBB staining.

(G) *In vivo* phosphorylation levels of HsfA1d by BIN2 kinase in a Phos-tag mobility shift assay. The GFP-HsfA1d proteins were immunoprecipitated from total active proteins of *GFP-HsfA1d*/Col-0 and *GFP-HsfA1d/bin2-1* transgenic plants and treated with or without CIP. Proteins were separated by SDS-PAGE with or without Phos-tag and detected with GFP antibody. The numbers indicate the relative ratio of phosphorylated HsfA1d and unphosphorylated HsfA1d protein shifts. P-HsfA1d indicates phosphorylated HsfA1d, and HsfA1d indicates unphosphorylated HsfA1d.

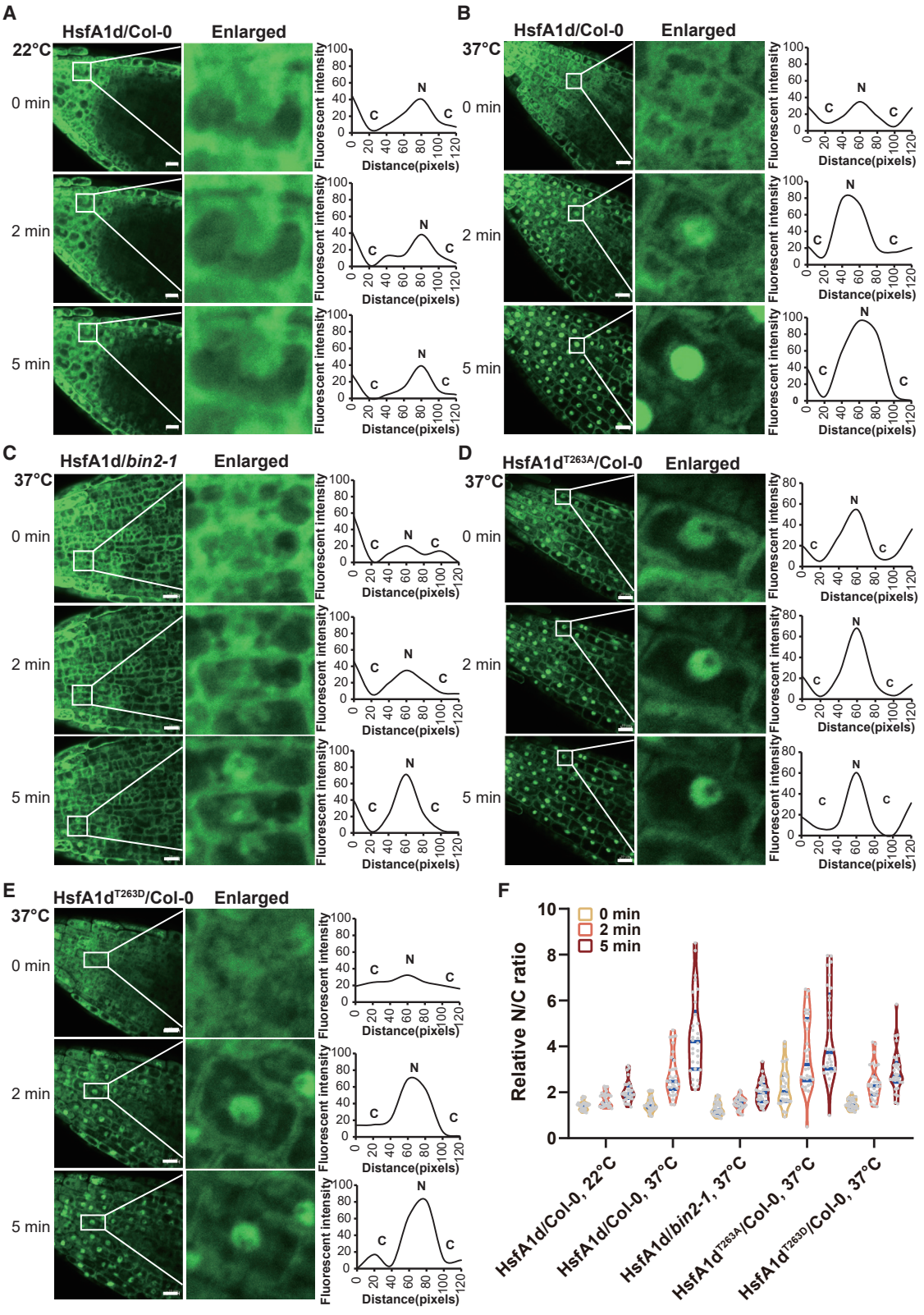

Figure 3. BIN2 inhibits the nuclear localization of HsfA1d

(A and B) Subcellular localization of GFP-HsfA1d in the Col-0 backgrounds in *Arabidopsis* root tip cells under **(A)** 22°C and **(B)** 37°C treatment for the indicated time. Scale bars, 10 μm. The relative fluorescence intensity of the nucleus and cytoplasm in the indicated cell was measured using ImageJ software. N, nucleus; C, cytoplasm.

(legend continued on next page)

influence its nuclear localization, which is required for the regulation of HSR gene expression (Yoshida et al., 2011). To answer this question, we used the transgenic plants *GFP-HsfA1d*/Col-0, *GFP-HsfA1d/bin2-1*, *GFP-HsfA1d*^{T263A}/Col-0, and *GFP-HsfA1d*^{T263D}/Col-0 to observe HsfA1d protein subcellular localization before and after HS treatment. Consistent with a previous report (Yoshida et al., 2011), the wild-type HsfA1d was localized to both the cytoplasm and nucleus under normal conditions but immediately accumulated in the nucleus upon 37°C treatment (Figures 3A, 3B, and 3F). This was a fast process, as the nuclear accumulation was triggered in just two minutes. We further tested the subcellular localization of HsfA1d in the *bin2-1* background and found that a higher level of HsfA1d protein was retained in the cytoplasm compared with the Col-0 background under normal temperature, and shuttling of the HsfA1d protein from the cytoplasm into the nucleus was inhibited in the *bin2-1* background upon 37°C treatment (Figures 3C and 3F). The HsfA1d^{T263A} form was observed to be localized largely in the nucleus, but the phosphomimic variant HsfA1d^{T263D} was retained mainly in the cytoplasm compared with the wild-type HsfA1d under normal temperature, and shuttling of HsfA1d^{T263D} protein from the cytoplasm to the nucleus also became more sluggish compared with the wild-type HsfA1d (Figures 3D–3F and supplemental figure 5). Taken together, these results demonstrated that BIN2 phosphorylates HsfA1d on T263 to suppress its accumulation in the nucleus at the early stage of the heat response.

BIN2 inhibits DNA-binding ability of HsfA1d by phosphorylating S56

Another phosphorylation site of HsfA1d by BIN2 kinase identified *in vitro* is S56, which is located in the DNA-binding domain and is conserved not only among the other members of the AtHsfA1s but also in most green plants (Figure 4A and supplemental figure 6). We therefore tested whether the phosphorylation of S56 by BIN2 affects the DNA-binding ability of HsfA1d. HsfA1d can bind to HSEs in the *HSP18.2* promoter to regulate its transcription *in vivo* (Yoshida et al., 2011), so we synthesized biotin-labeled DNA sequences containing HSEs of the *HSP18.2* promoter to perform DNA pull-down assays. We checked the DNA-binding ability of HsfA1d by biotin immunoprecipitation and detection of HsfA1d-His proteins. We found that the DNA-binding ability of HsfA1d was dramatically reduced in the presence of BIN2 and ATP, whereas the kinase-dead form BIN2^{K69R} had no effect (Figure 4B), suggesting a phosphorylation-dependent inhibition of DNA binding. To detect the HsfA1d DNA-binding activity *in vivo*, we next performed chromatin immunoprecipitation followed by quantitative PCR (ChIP-qPCR) assays using *GFP-HsfA1d/bin2-1* and the control line *GFP-HsfA1d*/WT. After ChIP with GFP antibody, we detected enrichment of the *HSP18.2* promoter and found that the enrichment was significantly reduced in *GFP-HsfA1d/bin2-1* plants compared with *GFP-HsfA1d*/WT plants (Figure 4C), suggesting the inhibition of DNA binding by BIN2 phosphorylation. To study the effect of S56 phosphorylation on DNA-binding ability, we performed DNA pull-down assays using HsfA1d, HsfA1d^{S56A}, and HsfA1d^{S56D} proteins. We found that the binding of HsfA1d^{S56A} to the *HSP18.2* promoter was similar to that of the wild-type HsfA1d, but the binding of HsfA1d^{S56D} was largely repressed (Figure 4D).

To further investigate whether the weakened DNA-binding ability of HsfA1d by BIN2 phosphorylation can directly affect its transcriptional regulation of downstream genes, we performed transient transactivation assays in *Arabidopsis* mesophyll protoplasts using a dual-luciferase reporter system. We fused the coding sequence (CDS) of *HsfA1d* to *eGFP* as the effector plasmid *35S:HsfA1d-eGFP*, and *35S:eGFP* was used as the control. An approximately 900-bp region containing HSEs of the *HSP18.2* promoter was fused with the *Luciferase* (*LUC*) gene to make a reporter. The *Renilla luciferase* (*REN*) gene was linked and driven by a *35S* promoter to serve as a control for normalization in the reporter plasmid *35:REN-P*$_{HSP18.2}$*-LUC* (Figure 4E). We introduced the reporter and effector plasmids into protoplasts of *bin2-3/bil1/bil2*, *bin2-1*, and their corresponding WTs. The LUC/REN ratio was significantly increased in *bin2-3/bil1/bil2* compared with Ws-2 (Figure 4F), whereas it was markedly reduced in *bin2-1* compared with the WT (Figure 4G). To further investigate whether the inhibition of HsfA1d transcriptional activity by BIN2 is due to S56 phosphorylation, we subsequently mutated S56 to Ala and Asp in effector plasmids and performed similar dual-luciferase transcription activity assays in protoplasts. We found that the LUC/REN ratio in *35S:HsfA1d*^{S56A}*-eGFP* was not significantly different from that in *35S:HsfA1d-eGFP* but was significantly lower in *35S:HsfA1d*^{S56D}*-eGFP* (Figure 4H). Moreover, we found that BIN2 also inhibits the DNA-binding and transactivation ability of HsfA1b (supplemental figure 7). Taken together, these data support a scenario in which BIN2 inhibits the DNA-binding ability of HsfA1d to suppress HSR gene transcription by phosphorylating the conserved S56 residue.

BIN2 functions upstream of HsfA1d to inhibit *Arabidopsis* thermotolerance

To verify whether the phosphorylation of HsfA1d by BIN2 can influence *Arabidopsis* thermotolerance, we performed a thermotolerance assay using the transgenic plants *GFP-HsfA1d*/Col-0, *GFP-HsfA1d*^{T263A}/Col-0, and *GFP-HsfA1d*^{T263D}/Col-0, which overexpressed similar amounts of different forms of HsfA1d (Figures 5A–5C). We found that *GFP-HsfA1d*/Col-0, which overexpressed the wide-type form of HsfA1d, had a higher survival rate than Col-0 (Figures 5A and 5B). The survival rate of *GFP-HsfA1d*^{T263A}/Col-0 did not differ significantly from that of *GFP-HsfA1d*/Col-0. However, *GFP-HsfA1d*^{T263D}/Col-0 had a significantly lower survival rate

(C) Subcellular localization of GFP-HsfA1d in the *bin2-1* backgrounds in *Arabidopsis* root tip cells under 37°C treatment for the indicated time. Scale bars, 10 μm. The relative fluorescence intensity of the nucleus and cytoplasm in the indicated cell was measured using ImageJ software. N, nucleus; C, cytoplasm.

(D and E) Subcellular localization of **(D)** GFP-HsfA1d^{T263A} and **(E)** GFP-HsfA1d^{T263D} in the Col-0 backgrounds in *Arabidopsis* root tip cells under 37°C treatment for the indicated time. Scale bars, 10 μm. The relative fluorescence intensity of the nucleus and cytoplasm in the indicated cell was measured using ImageJ software. N, nucleus; C, cytoplasm.

(F) Statistical analysis of the relative fluorescence intensity of the nucleus and cytoplasm in root tip cells of transgenic *Arabidopsis*. At least 30 cells randomly selected from 5 root tips per line were measured.

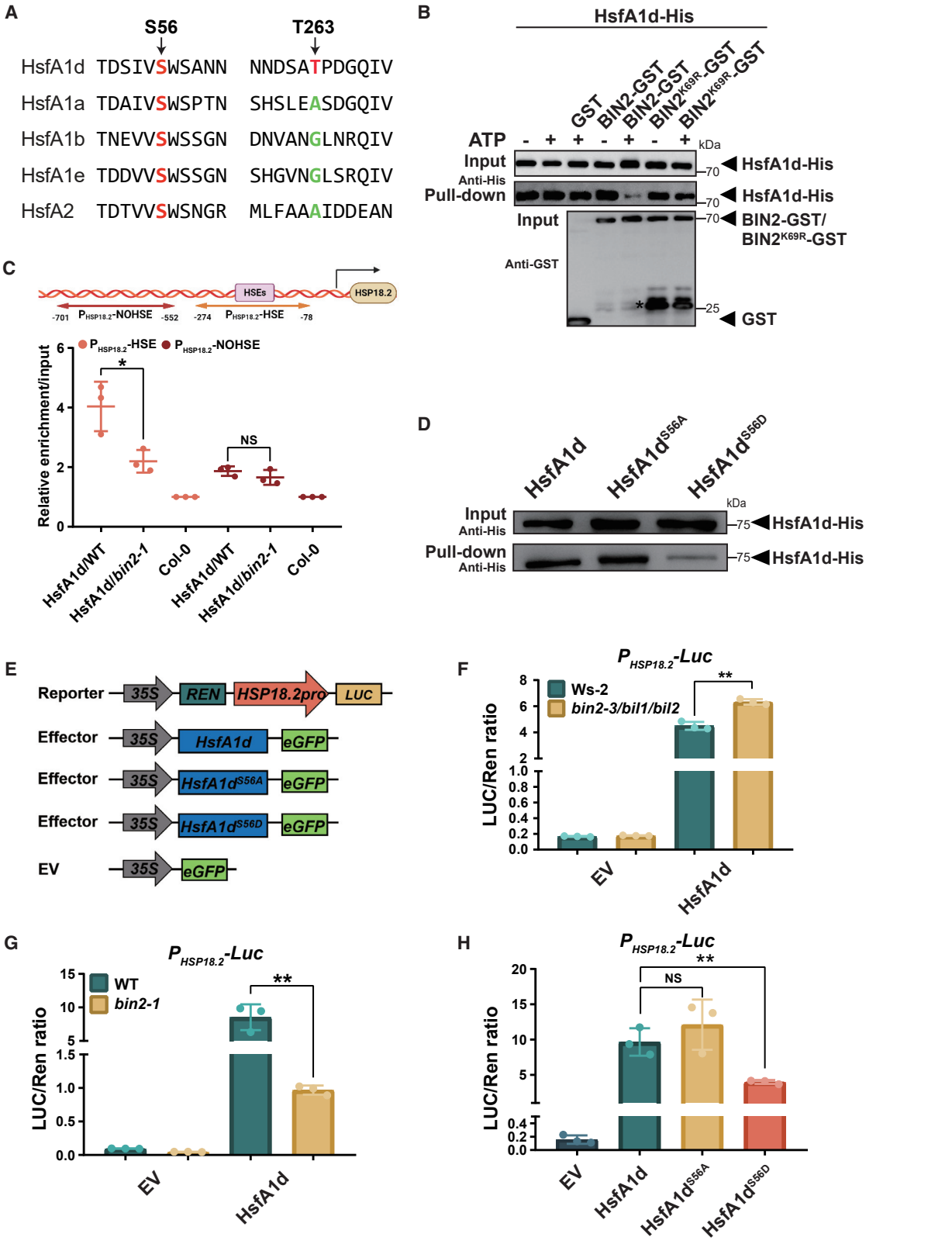

Figure 4. BIN2 inhibits the DNA-binding ability of HsfA1d by phosphorylating S56

(A) The alignment of HsfA1 and HsfA2 sequences surrounding S56 and T263 of HsfA1d in *Arabidopsis*.

(legend continued on next page)

compared with *GFP-HsfA1d*/Col-0 and *GFP-HsfA1d*^{T263A}/Col-0 (Figures 5A and 5B). These results demonstrated that the phosphorylation of T263 on HsfA1d can influence *Arabidopsis* thermotolerance. To further explore the genetic relationship between BIN2 and HsfA1d, we performed a thermotolerance assay using the HsfA1a, HsfA1b, and HsfA1d triple-knockout mutant *hsfa1a/b/d* (Liu et al., 2011) treated with bikinin, which is a chemical inhibitor of *Arabidopsis* GSK3-like kinases (De Rybel et al., 2009). We found that bikinin treatment significantly promoted the survival rates of Col-0 and Ws-2 but did not promote the survival rate of *hsfa1a/b/d*, compared with DMSO treatment (Figures 5D and 5E). These results demonstrated that the inhibition of *Arabidopsis* thermotolerance by BIN2 depends on its regulation of HsfA1d, and BIN2 functions upstream of HsfA1d.

BRs promote plant thermotolerance by regulating HsfA1d

Exogenous application of eBL has been shown to increase the survival rates of *Arabidopsis* seedlings under heat stress (Kagale et al., 2007). To investigate whether BRs promote plant thermotolerance by regulating HsfA1d through BIN2, we first checked the effect of eBL on the phosphorylation level of HsfA1d by performing Phos-tag mobility shift assays using*GFP-HsfA1d*/Col-0 transgenic plants with or without eBL treatment. We found that compared with the control, heat treatment and eBL treatment both promoted the relative amount of dephosphorylated HsfA1d protein. Bikinin treatment, which inhibited the BIN2 kinase, also promoted the relative amount of dephosphorylated HsfA1d protein (Figure 6A). These results indicated that BRs promote the dephosphorylation of HsfA1d *in vivo*. We further tested the subcellular localization of GFP-HsfA1d under eBL treatment and found that compared with the DMSO treatment, GFP-HsfA1d accumulated quickly in the nucleus of root tip cells after eBL treatment, as soon as two minutes, similar to the effect of 37°C treatment (Figures 6B, 6C, and 6E). To further investigate whether BR-promoted nuclear localization of HsfA1d is mediated by BIN2, we used *GFP-HsfA1d*/Col-0 and *GFP-HsfA1d/bin2-1* to compare the subcellular localization of GFP-HsfA1d before and after eBL treatment. We found that GFP-HsfA1d did not accumulate in the nucleus in the *bin2-1* background after eBL treatment (Figures 6D and 6E). We also performed transient transactivation assays by co-expressing the reporter plasmid *35S:REN-P$_{HSP18.2}$-LUC* and the effector plasmid *35S:HsfA1d-eGFP* in Col-0 protoplasts. The LUC/REN ratio was significantly increased by eBL treatment, and this facilitation by eBL was abolished in *bin2-1* protoplasts (Figure 6F). Taken together, these results indicated that BR promotes the activation of HsfA1d for HSR gene expression.

DISCUSSION

In this study, we revealed that BR promotes plant thermotolerance in early HSRs by regulating the phosphorylation of HsfA1s through the BR signaling component BIN2. From our thermotolerance assays, we found that the BR-deficient mutants and early signaling-attenuated mutants had lower survival rates under HS treatment. However, the survival rate of a *BES1* knockdown line was not significantly different from that of the WT (Figure 1). Apparently, the downstream component BES1 does not take part in BR-mediated thermotolerance in *Arabidopsis*. It is likely that BR signaling regulates plant thermomorphogenesis and thermotolerance using different downstream transcriptional machineries.

Furthermore, we provided several lines of evidence to demonstrate that BIN2 interacts with HsfA1b and HsfA1d and phosphorylates most members of the HsfA1s, especially HsfA1d, *in vitro* and *in vivo* (Figure 2). We further found that BIN2 phosphorylates HsfA1d on T263 to suppress its nuclear translocation (Figure 3). In addition, BIN2 inhibits the DNA-binding ability of HsfA1d to suppress HSR gene transcription by phosphorylating its S56 residue, which is conserved among the HsfA1s (Figure 4). Moreover, BIN2 functions upstream of HsfA1d to inhibit plant thermotolerance (Figure 5). Finally, we demonstrated that BRs promote plant thermotolerance by inhibiting BIN2 to activate HsfA1d for early HSRs (Figure 6).

On the basis of our findings, BIN2 plays a central role in negatively regulating plant thermotolerance by inhibiting HsfA1d, a master transcriptional activator in early HSRs. We thus propose a model that explains how BR promotes plant thermotolerance through its signaling pathway in *Arabidopsis* (Figure 7). When BR is absent, BIN2 phosphorylates HsfA1d on T263 and S56 to suppress its nuclear localization and DNA-binding activity, respectively. The HSR is reduced as a result of these events (Figure 7A). In the presence of BRs, the BIN2-mediated inhibition is immediately released to facilitate the nuclear accumulation and DNA-binding ability of HsfA1d to promote HSRs (Figure 7B).

A recent report showed that BES1 is dephosphorylated and activated independently of BR signaling but partially by abscisic acid (ABA)-repressed PP2C-type phosphatases after at least one hour of heat stress treatment, demonstrating that BES1 mediates the

(B) DNA–protein pull-down assays of HsfA1d protein with the *HSP18.2* promoter. A DNA fragment (−274 to −78) containing the HSEs of the *HSP18.2* promoter was used to generate biotin-labeled primers. HsfA1d-His and BIN2-GST or BIN2^{K69R}-GST proteins were incubated in kinase reaction buffer as indicated. The kinase reaction products were added to biotin-labeled DNA-bead mixes for binding. Asterisks indicate nonspecific bands.
(C) ChIP-qPCR assays quantifying the relative enrichment of the *HSP18.2* promoter precipitated with GFP-HsfA1d in seedlings from WT and *bin2-1* backgrounds. P$_{HSP18.2}$-HSE indicates the DNA fragment that contains HSEs of the *HSP18.2* promoter (−274 to −78), and P$_{HSP18.2}$-NOHSE indicates the DNA fragment with no HSEs from the *HSP18.2* promoter (−701 to −552). Data are mean ± SD (n = 3 biological replicates). p values were determined using unpaired t tests (*p < 0.05).
(D) DNA–protein pull-down assays of HsfA1d, HsfA1d^{S56A}, and HsfA1d^{S56D} proteins with the *HSP18.2* promoter.
(E) Schematic diagrams of luciferase reporter and effector constructs used in transient transactivation assays in *Arabidopsis* mesophyll protoplasts.
(F and G) Expression of *P$_{HSP18.2}$-LUC* in *bin2-3/bil1/bil2* **(F)**, *bin2-1* **(G)**, and their corresponding WT protoplasts with or without expression of *HsfA1d*. Data are mean ± SD (n = 3 biological replicates). p values were determined using Student's t test (**p < 0.01).
(H) Expression of *P$_{HSP18.2}$-LUC* in Col-0 protoplasts with the expression of *HsfA1d*, *HsfA1d^{S56A}*, or *HsfA1d^{S56D}*. Data are mean ± SD (n = 3 biological replicates). p values were determined using Student's t test (**p < 0.01).

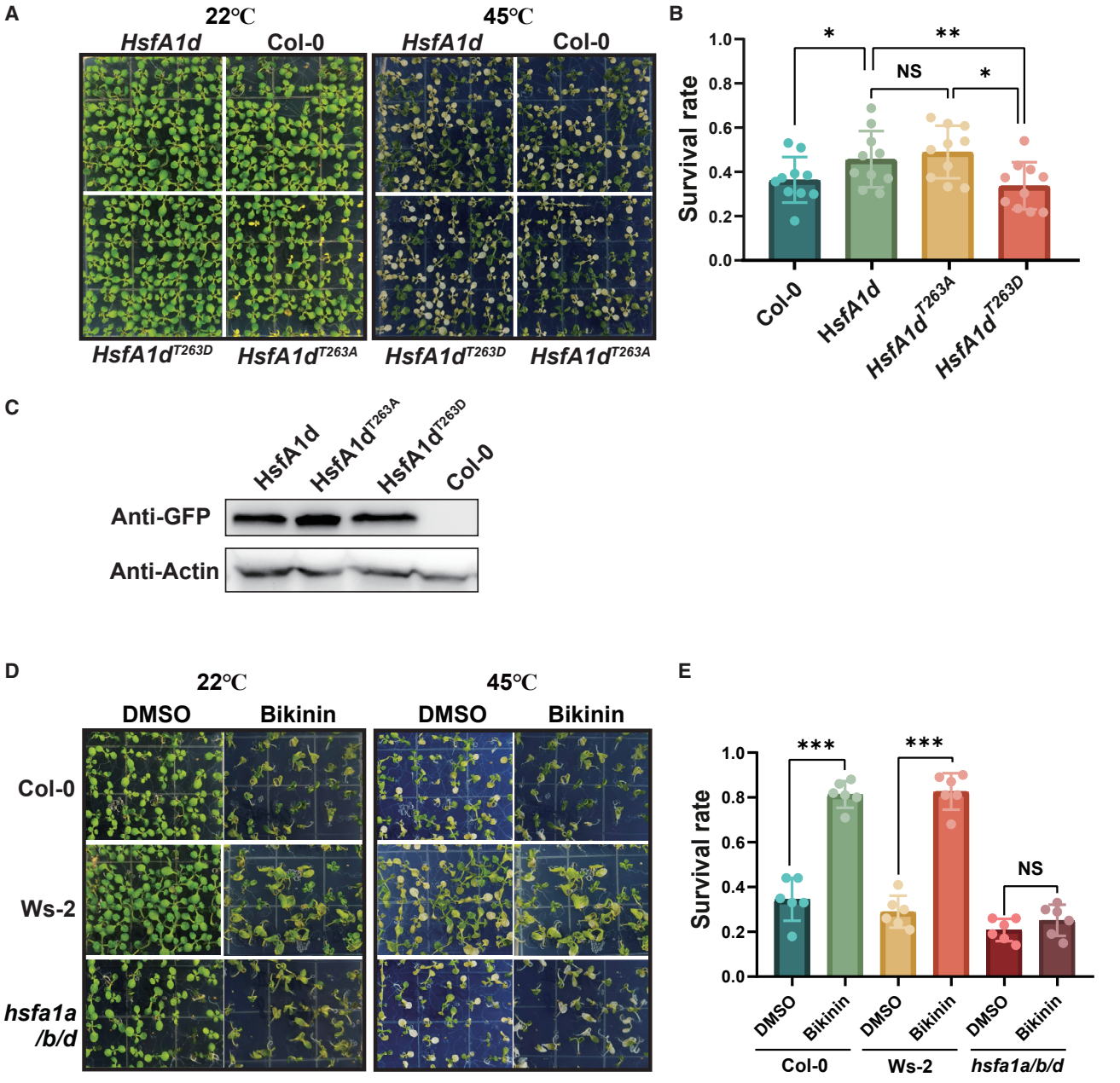

Figure 5. BIN2 inhibits *Arabidopsis* thermotolerance by regulating HsfA1d

(A) Basal thermotolerance phenotypes of the *Arabidopsis* transgenic materials *GFP-HsfA1d*/Col-0, *GFP-HsfA1d*^{T263A}/Col-0, and *GFP-HsfA1d*^{T263D}/Col-0. Nine-day-old seedlings were treated at 45°C for 105 min, followed by a 4-day recovery at 22°C.

(B) Statistical analysis of thermotolerance phenotypes. The survival rates were calculated after 45°C treatment and recovery. Each plate was considered to be one biological replicate, and at least 10 biological replicates collected from three to four independent experiments were used for statistical analysis of survival rate. Data are mean ± SD (n = 10). p values were determined using paired t tests (*$p < 0.05$ and **$p < 0.01$; non-significant [NS], $p > 0.05$).

(C) Protein quantification of GFP-HsfA1d protein in the *Arabidopsis* transgenic materials *GFP-HsfA1d*/Col-0, *GFP-HsfA1d*^{T263A}/Col-0, and *GFP-HsfA1d*^{T263D}/Col-0.

(D) Basal thermotolerance phenotype of the triple-knockout mutant *hsfa1a/b/d* and the WT with or without bikinin treatment. Nine-day-old seedlings grown on 1/2 MS plates with 0.01% DMSO or 20 μM bikinin were treated by 45°C for 105 min, followed by a 4-day recovery at 22°C.

(E) Statistical analysis of thermotolerance phenotypes. The survival rates were calculated after 45°C treatment and recovery. Each plate was considered to be one biological replicate, and at least 6 biological replicates were used for statistical analysis of survival rate. Data are mean ± SD (n = 6). p values were determined using paired t tests (***$p < 0.001$; non-significant [NS], $p > 0.05$).

crosstalk between prolonged HSRs and ABA signaling (Albertos et al., 2022). Our results showed that BIN2 directly regulates the activity of HsfA1d through post-translational modifications, and eBL immediately activates HsfA1d in early HSRs by inhibiting BIN2. These results demonstrated the critical role of BIN2 in mediating the crosstalk between early HSRs and BR signaling.

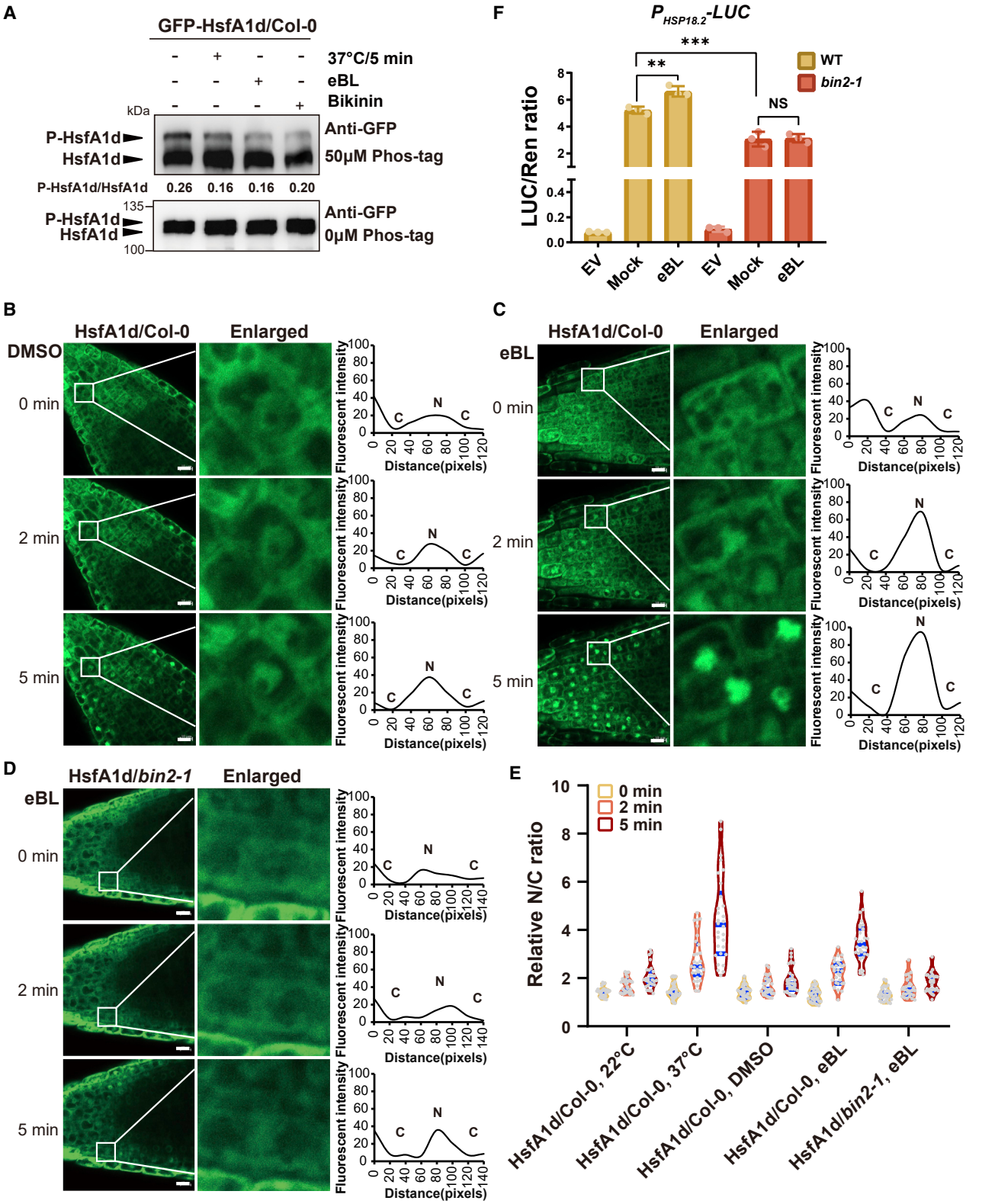

Figure 6. BRs promote plant thermotolerance by regulating HsfA1d

(A) Phosphorylation level of GFP-HsfA1d protein by *in vivo* Phos-tag assay. The GFP proteins immunoprecipitated from total active proteins of *GFP-HsfA1d*/Col-0 transgenic plants were separated by SDS-PAGE with or without Phos-tag and detected with GFP antibody. The numbers indicate the relative ratio of phosphorylated HsfA1d and unphosphorylated HsfA1d protein shifts.

(legend continued on next page)

We propose that plants may use different mechanisms at different heat shock stages to skillfully regulate HSRs, a possibility that is worthy of future investigation.

We also propose that BIN2 may be a hub that links heat stress with other abiotic stresses. Here, we found that BIN2 acts as an important and sophisticated regulator of HsfA1d activity to inhibit multiple functions of HsfA1d. In addition, BIN2 has been reported to act as a central component in many other abiotic stress signaling networks in plants (Cai et al., 2014; Jiang et al., 2019; He et al., 2021). For example, BIN2 phosphorylates and negatively regulates the stability of the transcription factor INDUCER OF CBF EXPRESSION (ICE1) in response to cold stress in *Arabidopsis* (Ye et al., 2019). Furthermore, heat stress can be closely related to other abiotic stresses such as drought, cold, and salt stresses, which have also been reported to regulate the function of BIN2 (Wang et al., 2018; Jiang et al., 2019; Ye et al., 2019; Li et al., 2020). To investigate whether heat stress regulates BR signaling or BIN2, we tested the dissociation of BKI1 from the plasma membrane under heat stress treatment using the *35S:BKI1-YFP* transgenic plants. We found that heat treatment did not trigger the dissociation of BKI1 from the plasma membrane (supplemental figure 8A), suggesting that heat stress does not activate early BR signaling to promote BKI1 dissociation from the plasma membrane. To investigate the effect of HS on BIN2, we checked the protein level of BIN2 after HS and found that BIN2-FLAG protein level accumulated after at least 30 min of HS treatment (supplemental figure 8B). We further detected the phosphorylation status of BES1, as it is largely dependent on the kinase activity of BIN2, using the *35S:BES1-FLAG* transgenic plants to indicate BIN2 activity. Compared with the phosphorylation level of BES1 in the absence of heat stress treatment, BES1 phosphorylation was almost unaffected within 30 min of heat stress treatment, although BES1 was dephosphorylated when the treatment was extended to 60 min (supplemental figure 8C). These results demonstrated that short-term (<10 min) HS has no obvious effect on BIN2 activity and stability. Therefore, whether and how HS regulates BR signaling and BIN2 requires further exploration.

The reversible phosphorylation of HSFs is a key step in regulating their activity for initiation of the HSR, a process that involves distinct protein kinases, phosphatases, and multiple phosphorylation sites. Human HSF1 can be phosphorylated and activated by calmodulin-dependent protein kinase II on S230 and by AKT1 on S326 (Holmberg et al., 2001; Lu et al., 2022). Other studies have reported that constitutive phosphorylation of HSF1 on S307 by MAP kinase and on S303 by GSK3β has an important role in the negative regulation of HSF1 DNA-binding and transcriptional activity at control temperatures (He et al., 1998; Xavier et al., 2000). This evidence indicates that phosphorylation is an important process that provides dynamic and elaborate tuning of HSF1 activity. Much evidence has indicated that similar mechanisms may exist in plants. It has been reported that the CaM-binding protein kinase CBK3 phosphorylates HsfA1a to promote the DNA-binding activity of HsfA1a in *Arabidopsis* (Liu et al., 2008). Here, we found that BIN2 phosphorylates the T263 and S56 sites of HsfA1d to inhibit its nuclear localization and DNA-binding activity, respectively (Figures 3 and 4). Moreover, we found that heat shock or eBL treatment reduces the overall phosphorylation level of HsfA1d *in vivo* (Figure 6A), which suggests that HsfA1d is activated largely through dephosphorylation. It is obvious that the activity of HsfA1s can be regulated by phosphorylation or dephosphorylation of different sites through multiple components, which leads to the production of HsfA1s with a variety of activities to enable accurate responses to diverse environmental conditions.

Heat stress causes a reduction in grain yield and quality by inhibiting plant metabolic and developmental processes that ultimately determine the production of grains. BRs play key roles in promoting broad aspects of plant growth and development by upregulating genes associated with cell division and elongation, cell wall synthesis, and photosynthesis, whose effects on biomass may be the most useful to develop in order to improve crop yields. Our research demonstrated that BRs promote thermotolerance by regulating BIN2 to activate the stress-resistance component HsfA1d. It is clear that fine-tuning the action of BR has the potential to increase cereal tolerance and acclimation to heat stress and thus maintain yields. Using CRISPR technology to generate plants with enhanced BR signaling or low BIN2 activity should be a practical way to design HS-resistant crops.

MATERIALS AND METHODS

Plant materials and growth conditions

Arabidopsis materials including various mutants, transgenic plants, and their corresponding wild types (WTs) used in this study are summarized in supplemental table 1. Columbia (Col-0) and Wassilewskija (Ws-2) were used as the WTs. The mutants *det2-1*, *DWF4-OX*, *bri1-116*, *BRI1-OX*, *bin2-1*, *BES1-RNAi*, and *bes1-D* are in the Col-0 background, whereas *bin2-3/bil1/bil2* is in the Ws-2 background, and *hsfa1a/b/d* is in the Col-0 and Ws-2 background (Liu et al., 2011). Unless noted, seeds were surface-sterilized and sown on MS plates (0.8% agar, 0.5× Murashige and Skoog [MS] basal salt mixture, and 1% [m/v] sucrose [pH 5.8]). The seeds were stratified at 4°C for 3 days before transferring to a growth chamber (Percival) at 22°C under long-day light conditions (16 h light/8 h dark). After 7 days, the seedlings were transplanted into soil and grown in a greenhouse at 22°C under long-day light conditions (16 h light/8 h dark). *Nicotiana benthamiana* plants were grown in a greenhouse under 16 h light/8 h dark cycles at 28°C.

(B and C) Subcellular localization of GFP-HsfA1d in *Arabidopsis* root tip cells in the Col-0 background under **(B)** DMSO or **(C)** 1 μM eBL treatment. Scale bars, 10 μm. The relative fluorescence intensity of the nucleus and cytoplasm in the indicated cell was measured using ImageJ software. N, nucleus; C, cytoplasm.

(D) Subcellular localization of GFP-HsfA1d in *Arabidopsis* root tip cells in the *bin2-1* background under 1 μM eBL treatment. Scale bars, 10 μm. The relative fluorescence intensity of the nucleus and cytoplasm in the indicated cell was measured using ImageJ software. N, nucleus; C, cytoplasm.

(E) Statistical analysis of the relative fluorescence intensity of the nucleus and cytoplasm in root tip cells of transgenic *Arabidopsis*. At least 30 cells randomly selected from 5 root tips per line were measured.

(F) Expression of $P_{HSP18.2}$-*LUC* in WT or *bin2-1* protoplasts with the expression of *HsfA1d* with/without eBL treatment. Data are mean ± SD (n = 3). p values were determined using Student's t test (**p < 0.01 and ***p < 0.001). At least three biological replicates were performed; a point represents a biological repetition.

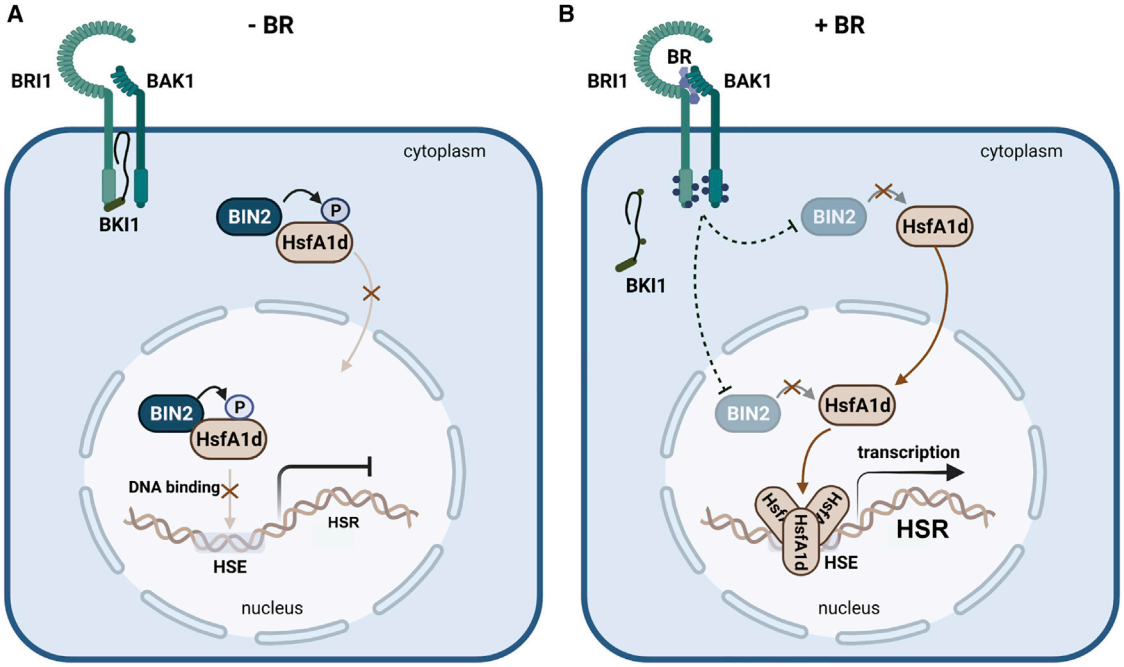

Figure 7. Proposed model of how BRs promote plant thermotolerance in *Arabidopsis*
(A) Without BRs, BIN2 phosphorylates HsfA1d on T263 and S56 to suppress its nuclear localization and DNA-binding ability, respectively, to inhibit HSRs.
(B) With BRs, BIN2 activity is inhibited, leading to nuclear accumulation and enhanced DNA-binding ability of HsfA1d to regulate HS-inducible gene expression, resulting in an enhanced HSR and elevated plant thermotolerance.

Thermotolerance assays

For thermotolerance assays, mutant and WT seeds were sterilized and sown on the same plates containing equal volumes of MS; the plates were poured on a leveling table to ensure the same conditions and minimize positional effects. After stratification at 4°C for 3 days, the plates were placed into a growth chamber (Percival) under 22°C and long-day light conditions (16 h light/8 h dark). After 9 days, the plates were transferred directly to a growth chamber (Percival) with the indicated high temperature and the same light conditions as the control for the indicated time; this was followed by a recovery period at 22°C for 4 days, after which the plates were photographed and assessed for survival rates. Survival was defined as the ability to maintain fresh and green leaves and to form new leaves.

For the thermotolerance assay with bikinin treatment, mutant and WT seeds were sterilized and sown on the same MS plates containing 20 μM bikinin (catalog #SML0094; Sigma) or 0.01% DMSO. The growth and heat treatment processes were the same as those described above.

Construction of plasmids and transgenic plants

For recombinant protein constructs, the CDSs of HsfA1a, HsfA1b, HsfA1d, HsfA1e, and BIN2 were cloned into the *pET28a*(+) vector to construct fusion proteins with a His-tag, and the CDSs of BIN2 and $BIN2^{K69R}$ (kinase-dead form of BIN2) were cloned into the *pGEX-4T-1* vector to construct fusion proteins with a GST-tag. For the BiFC assays, the cDNA sequences of HsfA1a, HsfA1b, HsfA1d, HsfA1e, and BES1 were fused with cYFP-tag flanked by the *35S* promoter into the *pXY104* vector, and the BIN2 cDNA sequence was fused with nYFP-tag flanked by the *35S* promoter into the *pXY106* vector. For the dual-luciferase reporter system, the CDS sequence of HsfA1d was cloned into a modified *pUC19* vector to construct the effector plasmid *35S:HsfA1d-eGFP*, and *pUC19* was used as the effector control. An approximately 900-bp region containing HSEs of the *HSP18.2* promoter was fused into the *pGreenII-0800-Luc* vector to construct the reporter plasmid *35:REN-*$P_{HSP18.2}$*-LUC*.

For transgenic plants, CDS sequences of the HsfA1s were cloned from Col-0 cDNA and fused into the *pCAMBIA1302* or modified *pCAMBIA1302* vectors to create *35S:HsfA1a-GFP*, *35S:HsfA1b-GFP*, *35S:HsfA1d-GFP*, *35S:HsfA1e-GFP*, *35S:GFP-HsfA1d*, *35S:GFP-*$HsfA1d^{T263A}$, and *35S:GFP-*$HsfA1d^{T263D}$ constructs. These constructs were transformed into *Agrobacterium tumefaciens* strain GV3101 before being transformed into *Arabidopsis* Col-0, *bin2-3/bil1/bil2*, or *bin2-1* using the floral dip method. Transgenic lines were selected on MS plates containing 35 μg/mL hygromycin B. Transgene expression was detected by western blotting with anti-GFP antibody (catalog #11814460001; Roche). *35S:BIN2-FLAG* transgenic plants were constructed in previous research (Cai et al., 2014). The sequences of all primers are listed in supplemental table 2.

Protein–protein interaction assays

For *in vitro* pull-down assays, HsfA1a-His, HsfA1b-His, HsfA1d-His, HsfA1e-His, GST, and BIN2-GST proteins were expressed in *Escherichia coli* strain *BL21*. Bacterial cells were incubated in 500 mL Luria-Bertani culture overnight and induced with 0.6 mM isopropyl β-D-thiogalactoside (IPTG). His-tagged and GST-tagged recombinant proteins were purified using TALON metal affinity resin (catalog #635501; Takara) and glutathione resin (catalog #L00206; GenScript), respectively. His-tagged and GST-tagged proteins were added to 36 μL buffer with 25 mM Tris (pH 7.4), 12 mM $MgCl_2$, and 1 mM DTT. The reaction mixture was incubated for 40 min at 37°C, then added to the glutathione resin beads and mixed with 500 μL GST-binding buffer (1× PBS, 0.01% Triton X- 100) for incubation at 4°C for 1 h. Then the reaction mixture was washed 6–8 times using GST-binding buffer. Finally, 5× SDS loading buffer was added to the resin beads, and the proteins were denatured by boiling at 95°C for 10 min before running on an SDS-PAGE gel and detection with anti-His antibody.

For BiFC assays, HsfA1a-cYFP, HsfA1b-cYFP, HsfA1d-cYFP, HsfA1e-cYFP, BES1-cYFP, and BIN2-nYFP constructs were transformed into *Agrobacterium tumefaciens* strain GV3101. The same amount (OD: 1.0) of agrobacteria cells were infiltrated into *Nicotiana benthamiana* leaves with

infiltration buffer (0.01 M MES, 10 mM $MgCl_2$, 0.2 mM acetosyringone). The plants were then placed in the dark for 24 h and grown under long-day conditions (16 h light/8 h dark) for 24–36 h at 28°C. Fluorescence signals in pavement cells were visualized by confocal microscopy (Leica).

For Co-IP assays, the transgenic plants *35S:HsfA1a-GFP*× *35S:BIN2-FLAG*, *35S:HsfA1b-GFP*× *35S:BIN2-FLAG*, *35S:HsfA1d-GFP*× *35S:BIN2-FLAG*, *35S:HsfA1e-GFP*× *35 S:BIN2-FLAG*, *35S:HsfA1a-GFP*, *35S:HsfA1b-GFP*, *35S:HsfA1d-GFP*, *35S:HsfA1e-GFP*, and *35S:BIN2-FLAG* were grown on soil for 12 days. Plant materials were ground into powder using liquid nitrogen and solubilized with 2× protein extraction buffer (100 mM Tris-HCl [pH 7.5], 300 mM NaCl, 2 mM EDTA [pH 8.0], 1% Triton X-100, 10% glycerol, and protease inhibitor). Extracts were centrifuged at 12 000 rpm for 10 min at 4°C, and the resulting supernatants were collected and incubated with GFP beads (catalog #KTSM1301; KTSM) at 4°C for 2 h. Beads were washed about three times with wash buffer, then boiled with 1× SDS loading buffer at 95°C for 10 min, and proteins were separated by SDS-PAGE and immunoblotted with anti-FLAG (catalog #F7425; Sigma) and anti-GFP (catalog #11814460001; Roche) antibodies.

In vitro kinase assay

For *in vitro* kinase assays, 0.2 μg BIN2-GST (used in Figure 2D) or BIN2-His (used in Figure 2F) proteins were incubated with 0.5 μg HsfA1a-His, HsfA1b-His, HsfA1d-His, and HsfA1e-His proteins in 36 μL kinase reaction buffer at 37°C for 40 min. The kinase reaction buffer was composed of 25 mM Tris (pH 7.4), 12 mM $MgCl_2$, 1 mM DTT, 0.1 mM ATP, and 0.5 μL (10 μCi) [γ-^{32}P] ATP. 5× SDS loading buffer was added to terminate the reaction. Samples were denatured by boiling at 95°C for 10 min before running SDS-PAGE.

Identifying phosphorylation sites of HsfA1s by BIN2 kinase

To verify the potential phosphorylation sites *in vitro*, 2 μg HsfA1a-His, HsfA1b-His, and HsfA1d-His and 0.2 μg BIN2-GST proteins were used in each kinase reaction, and the kinase reaction buffer was composed of 25 mM Tris (pH 7.4), 12 mM $MgCl_2$, 1 mM DTT, and 1 mM ATP. Recombinant proteins were incubated at 37°C for 2 h, and 5× SDS loading buffer was added to terminate the reaction. Samples were denatured by boiling at 95°C for 10 min and used for SDS-PAGE. Pieces of the SDS-PAGE gel containing the phosphorylated HsfA1 proteins were cut off for an in-solution alkylation/tryptic digestion followed by liquid chromatography-tandem mass spectrometry (LC-MS/MS) analysis to identify the potential phosphorylation sites, as described previously (Cai et al., 2014).

To verify the potential phosphorylation sites *in vivo*, seeds of the *35S:GFP-HsfA1d/bin2-1* transgenic plants were sterilized and sown on MS plates and cultivated in growth chambers as described above. After 9 days, homozygous seedlings of *35S:GFP-HsfA1d/bin2-1* and *35S:GFP-HsfA1d*/Col-0 were transplanted into soil and cultivated in a greenhouse at 22°C under long-day light conditions (16 h light/8 h dark). After 11 days, seedlings were collected and ground into fine powder. GFP-HsfA1d proteins were immunoprecipitated using GFP beads (catalog #KTSM1301; KTSM) after being extracted with protein extraction buffer (100 mM Tris-HCl [pH 7.5], 300 mM NaCl, 2 mM EDTA [pH 8.0], 1% Triton X-100, 10% glycerol, 100 mM PMSF, 25 μM MG132, protease inhibitor cocktail [catalog #P8340; Sigma], and PhosStop [catalog #04906845001; Roche]). Beads were washed about three times with wash buffer, then boiled with 1× SDS loading buffer at 95°C for 10 min, and proteins were separated by SDS-PAGE and stained with Coomassie brilliant blue. The input was immunoblotted with anti-GFP antibodies. Then SDS-PAGE gels that contained the GFP-HsfA1d proteins were collected and analyzed using LC-MS/MS.

In vivo Phos-tag mobility shift assay

For the *in vivo* Phos-tag mobility shift assay, total proteins from the *35S:GFP-HsfA1d*/Col-0 and *35S:GFP-HsfA1d/bin2-1* transgenic plants and Col-0 were immunoprecipitated using GFP beads. The Phos-tag mobility shift assay was performed as described in the Phos-tag SDS-PAGE guidebook. Total proteins were separated on an 8% (w/v) Phos-tag SDS-PAGE gel (50 μM Phos-tag and 0.1 mM $MnCl_2$; catalog #871839-54-2; Wako) or an 8% (w/v) regular SDS-PAGE gel. After electrophoresis, the Phos-tag SDS-PAGE gel was immersed in transfer buffer containing 10 mM EDTA and shaken gently two times for 20 min each. Then the Phos-tag SDS-PAGE gel was immersed in transfer buffer without EDTA and shaken gently for 10 min before being transferred to a PVDF blotting membrane. For CIP (catalog #M0525S; NEB) treatment, proteins were extracted with 2× protein extraction buffer and immunoprecipitated using GFP beads; CIP and the reaction buffer were added to the protein bead mixture and incubated at 37°C with gentle shaking. Then the samples were separated by SDS-PAGE as described above.

In vitro DNA pull-down assay

A 200-bp DNA sequence containing double-stranded perfect HSEs within the *HSP18.2* promoter was amplified using biotin-labeled primer pairs. The PCR products were purified with NaAc and ethyl alcohol. HsfA1d-His, HsfA1d^{T263A}-His, HsfA1d^{T263D}-His, GST, BIN2-GST, and BIN2^{K69R}-GST were expressed in *E. coli* BL21 and purified as described above. HsfA1d-His (2 μg) and 0.2 μg GST or BIN2-GST or BIN2^{K69R}-GST were used in each kinase reaction, with or without ATP in the kinase reaction buffer. Kinase reactions were performed at 37°C for 2 h. At the same time, 2 μg biotin-labeled double-stranded PCR products were added to 20 μL streptavidin MagBeads (catalog #L00424; GenScript) in 100 μL TES binding buffer (0.01 M Tris, 1 mM EDTA, 2 M NaCl), bound at room temperature for 1 h, and washed 3 times with IP buffer (0.1 M L-glutamic acid monopotassium salt monohydrate, 0.05 M Tris [pH 7.5], 2 mM $MgCl_2$, 0.05% [w/v] NP-40). Some kinase reaction products (10 μL) were removed as input, and the rest of the reaction products were added to DNA-bead mixes in 500 μL IP buffer for binding at 4°C for 2 h. Finally, 5× SDS loading buffer was added to the bead mixes after washing 3 times with IP buffer, and the bead mixes were then denatured by boiling and separated by SDS-PAGE for detection with anti-His and anti-GST antibodies.

Chromatin immunoprecipitation followed by quantitative PCR

ChIP-qPCR assays were performed as described previously (Jiang et al., 2021). Seedlings of Col-0, *35S:GFP-HsfA1d*/Col-0, and *35S:GFP-HsfA1d/bin2-1* were grown vertically at 22°C under 16 h light/8 h dark conditions for two weeks. Two grams of the seedlings were harvested and ground into fine powder in liquid nitrogen. The powder was crosslinked by adding nuclei isolation buffer (10 mM HEPES [pH 8.0], 1 M sucrose, 5 mM KCl, 5 mM $MgCl_2$, 0.6% Triton X-100, 0.4 mM PMSF, and protease inhibitor cocktail) with 1% formaldehyde and rotated gently for 15 min at room temperature. Crosslinking was stopped by adding 125 mM glycine and shaking at 4°C for 15 min. The mixture was then filtered through 2 layers of Miracloth and centrifuged at 3000 × *g* for 20 min at 4°C. The pellet was suspended with 1 ml ChIP buffer 2 (10 mM Tris-HCl [pH 8.0], 0.25 M sucrose, 10 mM $MgCl_2$, 1% Triton X-100, 1 mM EDTA, 5 mM β-mercaptoethanol, and protease inhibitor cocktail), transferred to a 1.5-ml tube, and centrifuged at 12 000 × *g* for 10 min at 4°C. Then the pellet was suspended with 300 μL nuclear lysis buffer (50 mM Tris-HCl [pH 8.0], 10 mM EDTA, 1% SDS, 0.1 mM PMSF, and protease inhibitor cocktail) and kept on ice for 10 min before adding ChIP dilution buffer (1.1% Triton X-100, 16.7 mM Tris-HCl [pH 8.0], 1.2 mM EDTA, 167 mM NaCl, 0.1 mM PMSF, and protease inhibitor cocktail) to 1 mL. The mixture was transferred to a sonication tube (500 μL/tube), then sonicated for 7 cycles with high frequency (Bioruptor Plus) and centrifuged at the maximum for 10 min. The supernatant was incubated with 30 μL anti-GFP beads overnight with rotation at 4°C (20 μL supernatant was removed as input). Then the bead mixture was sequentially washed with low-salt buffer (20 mM Tris-HCl [pH 8.0], 150 mM NaCl, 0.1% SDS, 1% Triton X-100, 2 mM EDTA), high-salt buffer (20 mM Tris-HCl [pH 8.0], 500 mM NaCl, 0.1% SDS, 1% Triton X-100, 2 mM EDTA), LiCl buffer (10 mM Tris-HCl [pH 8.0], 250 mM LiCl, 1% NP-40, 1% sodium deoxycholate, 1 mM EDTA), and TE buffer (10 mM Tris-HCl [pH 8.0] and 1 mM EDTA). The DNA–protein complex was eluted with ChIP elution buffer (1% SDS and 0.1 M $NaHCO_3$)

and shaken at 65°C and 1000 rpm for 10 min (repeat elution). Then the DNA–protein complex was reverse-crosslinked with 0.2 M NaCl at 65°C and shaken for at least 6 h. EDTA (10 μL, 0.5 M), 20 μL 1 M Tris-HCl (pH 7.0), 1 μL protease K (20 μg/μL), and 1 μL RNase were added and incubated at 45°C for 1 h with 800-rpm shaking. DNA was purified using the standard phenol–chloroform method and used for further quantitative PCR analyses. Quantitative real-time PCR was performed on a CFX 384 real-time PCR detection system (Bio-Rad) using SYBR Green Supermix (catalog #Q711-03; Vazyme).

Transient transactivation assay

A dual-luciferase reporter system was used to perform the transient transactivation assays. Plasmids were constructed as described above. *Arabidopsis* mesophyll protoplasts were isolated as described previously (Yoo et al., 2007; Wu et al., 2009). Effector plasmids (1.7 μg) and 8.3 μg reporter plasmids were cotransformed into protoplasts and incubated for 12 h in the dark. For eBL treatment, 1 μM eBL (catalog #E1641; Sigma) was added to the protoplasts and incubated for 5 h before lysing. The reagents of the Dual-Luciferase Reporter Assay System (catalog #E1910; Promega) were used to lyse the protoplasts for preparing cell lysates and for sequential assays of firefly and *Renilla* luciferases. The luciferase activity was assayed using ELISA (Spark).

Gene expression analysis by reverse-transcription PCR

Seeds were sterilized and sown as described above. After 9 days, the plates were placed into a growth chamber under light conditions (16 h light/8 h dark) at 37°C for 0, 5, and 15 min; seedlings were then collected and ground to a fine powder with liquid nitrogen. Total RNA was extracted using TRIzol reagent. RNA samples were reverse transcribed using a first-strand cDNA synthesis kit (catalog #R212-01; Vazyme) and oligo (dT). Quantitative PCR experiments were performed on a CFX 96 real-time PCR detection system (Bio-Rad) using SYBR Green Supermix. The *Arabidopsis* U-box gene (AT5G15400) was used as the internal control.

Subcellular localization assay

For subcellular localization assays, seedlings were grown as described above. For the heat shock treatment, seedlings were removed from the plates and placed into a microscope heat carrier module that was preheated to 37°C, and root tips were scanned under a confocal microscope. For eBL treatment, the seedlings were removed from the plates and dipped in liquid MS growth medium (0.5× MS basal salt mixture and 1% sucrose [pH 5.8]) with or without 1 μM eBL (catalog #E1641; Sigma) for a corresponding time, and the root tips were scanned under a confocal microscope (Zeiss).

SUPPLEMENTAL INFORMATION

Supplemental information is available at *Plant Communications Online*.

FUNDING

This work was supported by grant 31661143024 from the National Natural Science Foundation of China (to X.W.) and grant 0120150092 from the Agricultural Research Outstanding Talents and Innovation Team of the Ministry of Agriculture (to X.W.).

AUTHOR CONTRIBUTIONS

J.L., J.J., and X.W. designed the research. J.L. and J.J. performed the experiments and data analysis. J.L., J.J., S.S., and X.W. wrote and edited the paper.

ACKNOWLEDGMENTS

We thank Yee-Yung Charng (Academia Sinica) for providing the *hsfa1a/b/d* triple mutant. We thank Leelyn Chong and Jie Hu (Henan University) for editing the draft. The model figure was created using BioRender.com. The authors declare no competing interests.

Received: February 15, 2022
Revised: July 10, 2022
Accepted: August 1, 2022
Published: August 3, 2022

REFERENCES

Albertos, P., Dündar, G., Schenk, P., Carrera, S., Cavelius, P., Sieberer, T., and Poppenberger, B. (2022). Transcription factor BES1 interacts with HSFA1 to promote heat stress resistance of plants. EMBO J. **41**, e108664.

Anckar, J., and Sistonen, L. (2011). Regulation of HSF1 function in the heat stress response: implications in aging and disease. Annu. Rev. Biochem. **80**:1089–1115.

Andrási, N., Pettkó-Szandtner, A., and Szabados, L. (2021). Diversity of plant heat shock factors: regulation, interactions, and functions. J. Exp. Bot. **72**:1558–1575.

Babbar, R., Karpinska, B., Grover, A., and Foyer, C.H. (2020). Heat-induced oxidation of the nuclei and cytosol. Front. Plant Sci. **11**:617779.

Bienz, M., and Pelham, H.R. (1987). Mechanisms of heat-shock gene activation in higher eukaryotes. Adv. Genet. **24**:31–72.

Bita, C.E., and Gerats, T. (2013). Plant tolerance to high temperature in a changing environment: scientific fundamentals and production of heat stress-tolerant crops. Front. Plant Sci. **4**:273.

Cai, Z., Liu, J., Wang, H., Yang, C., Chen, Y., Li, Y., Pan, S., Dong, R., Tang, G., Barajas-Lopez, J.d.D., et al. (2014). GSK3-like kinases positively modulate abscisic acid signaling through phosphorylating subgroup III SnRK2s in Arabidopsis. Proc. Natl. Acad. Sci. USA **111**:9651–9656.

Cheng, Y., Zhu, W., Chen, Y., Ito, S., Asami, T., and Wang, X. (2014). Brassinosteroids control root epidermal cell fate via direct regulation of a MYB-bHLH-WD40 complex by GSK3-like kinases. Elife **3**, e02525.

Chu, B., Soncin, F., Price, B.D., Stevenson, M.A., and Calderwood, S.K. (1996). Sequential phosphorylation by mitogen-activated protein kinase and glycogen synthase kinase 3 represses transcriptional activation by heat shock factor-1. J. Biol. Chem. **271**:30847–30857.

Cui, Y., Lu, S., Li, Z., Cheng, J., Hu, P., Zhu, T., Wang, X., Jin, M., Wang, X., Li, L., et al. (2020). CYCLIC NUCLEOTIDE-GATED ION CHANNELs 14 and 16 promote tolerance to heat and chilling in rice. Plant Physiol. **183**:1794–1808.

De Rybel, B., Audenaert, D., Vert, G., Rozhon, W., Mayerhofer, J., Peelman, F., Coutuer, S., Denayer, T., Jansen, L., Nguyen, L., et al. (2009). Chemical inhibition of a subset of Arabidopsis thaliana GSK3-like kinases activates brassinosteroid signaling. Chem. Biol. **16**:594–604.

Deng, Y., Humbert, S., Liu, J.X., Srivastava, R., Rothstein, S.J., and Howell, S.H. (2011). Heat induces the splicing by IRE1 of a mRNA encoding a transcription factor involved in the unfolded protein response in Arabidopsis. Proc. Natl. Acad. Sci. USA **108**:7247–7252.

Dhaubhadel, S., Chaudhary, S., Dobinson, K.F., and Krishna, P. (1999). Treatment with 24-epibrassinolide, a brassinosteroid, increases the basic thermotolerance of Brassica napus and tomato seedlings. Plant Mol. Biol. **40**:333–342.

Evrard, A., Kumar, M., Lecourieux, D., Lucks, J., von Koskull-Döring, P., and Hirt, H. (2013). Regulation of the heat stress response in Arabidopsis by MPK6-targeted phosphorylation of the heat stress factor HsfA2. PeerJ **1**:e59.

Fang, Z., Ji, Y., Hu, J., Guo, R., Sun, S., and Wang, X. (2020). Strigolactones and brassinosteroids antagonistically regulate the stability of the D53-OsBZR1 complex to determine FC1 expression in rice tillering. Mol. Plant **13**:586–597.

Finka, A., Cuendet, A.F.H., Maathuis, F.J.M., Saidi, Y., and Goloubinoff, P. (2012). Plasma membrane cyclic nucleotide gated calcium channels control land plant thermal sensing and acquired thermotolerance. Plant Cell **24**:3333–3348.

Friedrich, T., Oberkofler, V., Trindade, I., Altmann, S., Brzezinka, K., Lämke, J., Gorka, M., Kappel, C., Sokolowska, E., Skirycz, A., et al. (2021). Heteromeric HSFA2/HSFA3 complexes drive transcriptional memory after heat stress in Arabidopsis. Nat. Commun. **12**:3426.

Gomez-Pastor, R., Burchfiel, E.T., and Thiele, D.J. (2018). Regulation of heat shock transcription factors and their roles in physiology and disease. Nat. Rev. Mol. Cell Biol. **19**:4–19.

Guo, L., Chen, S., Liu, K., Liu, Y., Ni, L., Zhang, K., and Zhang, L. (2008). Isolation of heat shock factor HsfA1a-binding sites in vivo revealed variations of heat shock elements in Arabidopsis thaliana. Plant Cell Physiol. **49**:1306–1315.

Guo, M., Liu, J.H., Ma, X., Luo, D.X., Gong, Z.H., and Lu, M.H. (2016). The plant heat stress transcription factors (HSFs): structure, regulation, and function in response to abiotic stresses. Front. Plant Sci. **7**:114.

Hao, Y., Wang, H., Qiao, S., Leng, L., and Wang, X. (2016). Histone deacetylase HDA6 enhances brassinosteroid signaling by inhibiting the BIN2 kinase. Proc. Natl. Acad. Sci. USA **113**:10418–10423.

Hayes, S., Schachtschabel, J., Mishkind, M., Munnik, T., and Arisz, S.A. (2021). Hot topic: thermosensing in plants. Plant Cell Environ. **44**:2018–2033.

He, B., Meng, Y.H., and Mivechi, N.F. (1998). Glycogen synthase kinase 3beta and extracellular signal-regulated kinase inactivate heat shock transcription factor 1 by facilitating the disappearance of transcriptionally active granules after heat shock. Mol. Cell Biol. **18**:6624–6633.

He, C., Gao, H., Wang, H., Guo, Y., He, M., Peng, Y., and Wang, X. (2021). GSK3-mediated stress signaling inhibits legume-rhizobium symbiosis by phosphorylating GmNSP1 in soybean. Mol. Plant **14**:488–502.

Higashi, Y., Ohama, N., Ishikawa, T., Katori, T., Shimura, A., Kusakabe, K., Yamaguchi-Shinozaki, K., Ishida, J., Tanaka, M., Seki, M., et al. (2013). HsfA1d, a protein identified via FOX hunting using Thellungiella salsuginea cDNAs improves heat tolerance by regulating heat-stress-responsive gene expression. Mol. Plant **6**:411–422.

Holmberg, C.I., Hietakangas, V., Mikhailov, A., Rantanen, J.O., Kallio, M., Meinander, A., Hellman, J., Morrice, N., MacKintosh, C., Morimoto, R.I., et al. (2001). Phosphorylation of serine 230 promotes inducible transcriptional activity of heat shock factor 1. EMBO J. **20**:3800–3810.

Hu, J., Ji, Y., Hu, X., Sun, S., and Wang, X. (2020). BES1 functions as the Co-regulator of D53-like SMXLs to inhibit BRC1 expression in strigolactone-regulated shoot branching in Arabidopsis. Plant Commun. **1**, 100014.

Jiang, H., Tang, B., Xie, Z., Nolan, T., Ye, H., Song, G.Y., Walley, J., and Yin, Y. (2019). GSK3-like kinase BIN2 phosphorylates RD26 to potentiate drought signaling in Arabidopsis. Plant J. **100**:923–937.

Jiang, J., Liu, J., Sanders, D., Qian, S., Ren, W., Song, J., Liu, F., and Zhong, X. (2021). UVR8 interacts with de novo DNA methyltransferase and suppresses DNA methylation in Arabidopsis. Nat. Plants **7**:184–197.

Jiang, J., Wang, T., Wu, Z., Wang, J., Zhang, C., Wang, H., Wang, Z.X., and Wang, X. (2015a). The intrinsically disordered protein BKI1 is essential for inhibiting BRI1 signaling in plants. Mol. Plant **8**:1675–1678.

Jiang, J., Zhang, C., and Wang, X. (2013). Ligand perception, activation, and early signaling of plant steroid receptor brassinosteroid insensitive 1. J. Integr. Plant Biol. **55**:1198–1211.

Jiang, J., Zhang, C., and Wang, X. (2015b). A recently evolved isoform of the transcription factor BES1 promotes brassinosteroid signaling and development in Arabidopsis thaliana. Plant Cell **27**:361–374.

Kagale, S., Divi, U.K., Krochko, J.E., Keller, W.A., and Krishna, P. (2007). Brassinosteroid confers tolerance in Arabidopsis thaliana and Brassica napus to a range of abiotic stresses. Planta **225**:353–364.

Kim, T.W., Guan, S., Burlingame, A.L., and Wang, Z.Y. (2011). The CDG1 kinase mediates brassinosteroid signal transduction from BRI1 receptor kinase to BSU1 phosphatase and GSK3-like kinase BIN2. Mol. Cell **43**:561–571.

Li, B., Gao, K., Ren, H., and Tang, W. (2018). Molecular mechanisms governing plant responses to high temperatures. J. Integr. Plant Biol. **60**:757–779.

Li, J., and Chory, J. (1997). A putative leucine-rich repeat receptor kinase involved in brassinosteroid signal transduction. Cell **90**:929–938.

Li, J., and Nam, K.H. (2002). Regulation of brassinosteroid signaling by a GSK3/SHAGGY-like kinase. Science **295**:1299–1301.

Li, J., Wen, J., Lease, K.A., Doke, J.T., Tax, F.E., and Walker, J.C. (2002). BAK1, an Arabidopsis LRR receptor-like protein kinase, interacts with BRI1 and modulates brassinosteroid signaling. Cell **110**:213–222.

Li, J., Zhou, H., Zhang, Y., Li, Z., Yang, Y., and Guo, Y. (2020). The GSK3-like kinase BIN2 is a molecular switch between the salt stress response and growth recovery in Arabidopsis thaliana. Dev. Cell **55**:367–380.e6.

Liu, H.-T., Gao, F., Li, G.-L., Han, J.-L., Liu, D.-L., Sun, D.-Y., and Zhou, R.-G. (2008). The calmodulin-binding protein kinase 3 is part of heat-shock signal transduction inArabidopsis thaliana. Plant J. **55**:760–773.

Liu, H.-T., Li, B., Shang, Z.-L., Li, X.-Z., Mu, R.-L., Sun, D.-Y., and Zhou, R.-G. (2003). Calmodulin is involved in heat shock signal transduction in wheat. Plant Physiol. **132**:1186–1195.

Liu, H.C., and Charng, Y.Y. (2013). Common and distinct functions of Arabidopsis class A1 and A2 heat shock factors in diverse abiotic stress responses and development. Plant Physiol. **163**:276–290.

Liu, H.C., Liao, H.T., and Charng, Y.Y. (2011). The role of class A1 heat shock factors (HSFA1s) in response to heat and other stresses in Arabidopsis. Plant Cell Environ. **34**:738–751.

Liu, H.T., Li, G.L., Chang, H., Sun, D.Y., Zhou, R.G., and Li, B. (2007). Calmodulin-binding protein phosphatase PP7 is involved in thermotolerance in Arabidopsis. Plant Cell Environ. **30**:156–164.

Liu, X., Yang, Q., Wang, Y., Wang, L., Fu, Y., and Wang, X. (2018). Brassinosteroids regulate pavement cell growth by mediating BIN2-induced microtubule stabilization. J. Exp. Bot. **69**:1037–1049.

Lu, W.C., Omari, R., Ray, H., Wang, J., Williams, I., Jacobs, C., Hockaden, N., Bochman, M.L., and Carpenter, R.L. (2022). AKT1 mediates multiple phosphorylation events that functionally promote HSF1 activation. FEBS J. **289**:3876–3893.

Mora-García, S., Vert, G., Yin, Y., Caño-Delgado, A., Cheong, H., and Chory, J. (2004). Nuclear protein phosphatases with Kelch-repeat domains modulate the response to brassinosteroids in Arabidopsis. Genes Dev. **18**:448–460.

Neill, E.M., Byrd, M.C.R., Billman, T., Brandizzi, F., and Stapleton, A.E. (2019). Plant growth regulators interact with elevated temperature to alter heat stress signaling via the Unfolded Protein Response in maize. Sci. Rep. **9**, 10392.

Nishizawa-Yokoi, A., Nosaka, R., Hayashi, H., Tainaka, H., Maruta, T., Tamoi, M., Ikeda, M., Ohme-Takagi, M., Yoshimura, K., Yabuta, Y., et al. (2011). HsfA1d and HsfA1e involved in the transcriptional regulation of HsfA2 function as key regulators for the Hsf signaling network in response to environmental stress. Plant Cell Physiol. **52**:933–945.

Nishizawa, A., Yabuta, Y., Yoshida, E., Maruta, T., Yoshimura, K., and Shigeoka, S. (2006). Arabidopsis heat shock transcription factor A2 as a key regulator in response to several types of environmental stress. Plant J. **48**:535–547.

Pelham, H.R.B. (1982). A regulatory upstream promoter element in the Drosophila hsp70 heat-shock gene. Cell **30**:517–528.

Qiao, S., Sun, S., Wang, L., Wu, Z., Li, C., Li, X., Wang, T., Leng, L., Tian, W., Lu, T., et al. (2017). The RLA1/SMOS1 transcription factor functions with OsBZR1 to regulate brassinosteroid signaling and rice architecture. Plant Cell **29**:292–309.

Sage, T.L., Bagha, S., Lundsgaard-Nielsen, V., Branch, H.A., Sultmanis, S., and Sage, R.F. (2015). The effect of high temperature stress on male and female reproduction in plants. Field Crop. Res. **182**:30–42.

Saidi, Y., Finka, A., Muriset, M., Bromberg, Z., Weiss, Y.G., Maathuis, F.J.M., and Goloubinoff, P. (2009). The heat shock response in moss plants is regulated by specific calcium-permeable channels in the plasma membrane. Plant Cell **21**:2829–2843.

Scharf, K.-D., Berberich, T., Ebersberger, I., and Nover, L. (2012). The plant heat stress transcription factor (Hsf) family: structure, function and evolution. Biochim. Biophys. Acta **1819**:104–119.

Shah, Z., Shah, S.H., Ali, G.S., Munir, I., Khan, R.S., Iqbal, A., Ahmed, N., and Jan, A. (2020). Introduction of Arabidopsis's heat shock factor HsfA1d mitigates adverse effects of heat stress on potato (Solanum tuberosum L.) plant. Cell Stress Chaperones **25**:57–63.

Sugio, A., Dreos, R., Aparicio, F., and Maule, A.J. (2009). The cytosolic protein response as a subcomponent of the wider heat shock response in Arabidopsis. Plant Cell **21**:642–654.

Sun, S., Chen, D., Li, X., Qiao, S., Shi, C., Li, C., Shen, H., and Wang, X. (2015). Brassinosteroid signaling regulates leaf erectness in Oryza sativa via the control of a specific U-type cyclin and cell proliferation. Dev. Cell **34**:220–228.

Tang, W., Kim, T.W., Oses-Prieto, J.A., Sun, Y., Deng, Z., Zhu, S., Wang, R., Burlingame, A.L., and Wang, Z.Y. (2008). BSKs mediate signal transduction from the receptor kinase BRI1 in Arabidopsis. Science **321**:557–560.

Volkov, R.A., Panchuk, I.I., Mullineaux, P.M., and Schöffl, F. (2006). Heat stress-induced H(2)O (2) is required for effective expression of heat shock genes in Arabidopsis. Plant Mol. Biol. **61**:733–746.

Wang, D., Yang, C., Wang, H., Wu, Z., Jiang, J., Liu, J., He, Z., Chang, F., Ma, H., and Wang, X. (2017). BKI1 regulates plant architecture through coordinated inhibition of the brassinosteroid and ERECTA signaling pathways in Arabidopsis. Mol. Plant **10**:297–308.

Wang, H., Tang, J., Liu, J., Hu, J., Liu, J., Chen, Y., Cai, Z., and Wang, X. (2018). Abscisic acid signaling inhibits brassinosteroid signaling through dampening the dephosphorylation of BIN2 by ABI1 and ABI2. Mol. Plant **11**:315–325.

Wang, H., Yang, C., Zhang, C., Wang, N., Lu, D., Wang, J., Zhang, S., Wang, Z.X., Ma, H., and Wang, X. (2011). Dual role of BKI1 and 14-3-3 s in brassinosteroid signaling to link receptor with transcription factors. Dev. Cell **21**:825–834.

Wang, J., Jiang, J., Wang, J., Chen, L., Fan, S.L., Wu, J.W., Wang, X., and Wang, Z.X. (2014a). Structural insights into the negative regulation of BRI1 signaling by BRI1-interacting protein BKI1. Cell Res. **24**:1328–1341.

Wang, L., Guo, Y., Jia, L., Chu, H., Zhou, S., Chen, K., Wu, D., and Zhao, L. (2014b). Hydrogen peroxide acts upstream of nitric oxide in the heat shock pathway in Arabidopsis seedlings. Plant Physiol. **164**:2184–2196.

Wang, X., and Chory, J. (2006). Brassinosteroids regulate dissociation of BKI1, a negative regulator of BRI1 signaling, from the plasma membrane. Science **313**:1118–1122.

Wang, X., Goshe, M.B., Soderblom, E.J., Phinney, B.S., Kuchar, J.A., Li, J., Asami, T., Yoshida, S., Huber, S.C., and Clouse, S.D. (2005a). Identification and functional analysis of in vivo phosphorylation sites of the Arabidopsis BRASSINOSTEROID-INSENSITIVE1 receptor kinase. Plant Cell **17**:1685–1703.

Wang, X., Li, X., Meisenhelder, J., Hunter, T., Yoshida, S., Asami, T., and Chory, J. (2005b). Autoregulation and homodimerization are involved in the activation of the plant steroid receptor BRI1. Dev. Cell **8**:855–865.

Wang, Y., Sun, S., Zhu, W., Jia, K., Yang, H., and Wang, X. (2013). Strigolactone/MAX2-induced degradation of brassinosteroid transcriptional effector BES1 regulates shoot branching. Dev. Cell **27**:681–688.

Wu, F.H., Shen, S.C., Lee, L.Y., Lee, S.H., Chan, M.T., and Lin, C.S. (2009). Tape-Arabidopsis Sandwich - a simpler Arabidopsis protoplast isolation method. Plant Methods **5**:16.

Xavier, I.J., Mercier, P.A., McLoughlin, C.M., Ali, A., Woodgett, J.R., and Ovsenek, N. (2000). Glycogen synthase kinase 3beta negatively regulates both DNA-binding and transcriptional activities of heat shock factor 1. J. Biol. Chem. **275**:29147–29152.

Xuan, Y., Zhou, S., Wang, L., Cheng, Y., and Zhao, L. (2010). Nitric oxide functions as a signal and acts upstream of AtCaM3 in thermotolerance in Arabidopsis seedlings. Plant Physiol. **153**:1895–1906.

Yamada, K., Fukao, Y., Hayashi, M., Fukazawa, M., Suzuki, I., and Nishimura, M. (2007). Cytosolic HSP90 regulates the heat shock response that is responsible for heat acclimation in Arabidopsis thaliana. J. Biol. Chem. **282**:37794–37804.

Yang, C.J., Zhang, C., Lu, Y.N., Jin, J.Q., and Wang, X.L. (2011). The mechanisms of brassinosteroids' action: from signal transduction to plant development. Mol. Plant **4**:588–600.

Yang, M., Li, C., Cai, Z., Hu, Y., Nolan, T., Yu, F., Yin, Y., Xie, Q., Tang, G., and Wang, X. (2017). SINAT E3 ligases control the light-mediated stability of the brassinosteroid-activated transcription factor BES1 in Arabidopsis. Dev. Cell **41**:47–58.e4.

Yang, M., and Wang, X. (2017). Multiple ways of BES1/BZR1 degradation to decode distinct developmental and environmental cues in plants. Mol. Plant **10**:915–917.

Ye, K., Li, H., Ding, Y., Shi, Y., Song, C., Gong, Z., and Yang, S. (2019). BRASSINOSTEROID-INSENSITIVE2 negatively regulates the stability of transcription factor ICE1 in response to cold stress in Arabidopsis. Plant Cell **31**:2682–2696.

Yin, Y., Wang, Z.Y., Mora-Garcia, S., Li, J., Yoshida, S., Asami, T., and Chory, J. (2002). BES1 accumulates in the nucleus in response to brassinosteroids to regulate gene expression and promote stem elongation. Cell **109**:181–191.

Yoo, S.D., Cho, Y.H., and Sheen, J. (2007). Arabidopsis mesophyll protoplasts: a versatile cell system for transient gene expression analysis. Nat. Protoc. **2**:1565–1572.

Yoshida, T., Ohama, N., Nakajima, J., Kidokoro, S., Mizoi, J., Nakashima, K., Maruyama, K., Kim, J.M., Seki, M., Todaka, D., et al. (2011). Arabidopsis HsfA1 transcription factors function as the main positive regulators in heat shock-responsive gene expression. Mol. Genet. Genomics. **286**:321–332.

Youn, J.H., and Kim, T.W. (2015). Functional insights of plant GSK3-like kinases: multi-taskers in diverse cellular signal transduction pathways. Mol. Plant **8**:552–565.

Zhao, C., Liu, B., Piao, S., Wang, X., Lobell, D.B., Huang, Y., Huang, M., Yao, Y., Bassu, S., Ciais, P., et al. (2017). Temperature increase reduces global yields of major crops in four independent estimates. Proc. Natl. Acad. Sci. USA **114**:9326–9331.